

Analysis and Testing of Methods to Determine Indoor Air Quality and Air Change Effectiveness

**Andreas Jung and Manfred Zeller
Rheinisch-Westfälische Technical University of Aachen
Aachen, Germany**

1994

Sponsored by:

**FLT – Research Federation for Air and Drying Technology
[FLT (Forschungsvereinigung für Luft- und Trocknungstechnik) e.V.]
VDMA Lyoner Straße 18
60528 Frankfurt am Main**

**English Translation:
Wolfgang Lukaschek
Center for the Built Environment (CBE)
University of California, Berkeley**

Table of Contents

1	Introduction.....	3
2	Principles for Determining Air Change Effectiveness	4
3	Realization of and Compliance with Measurement Boundary Conditions	8
3.1	General Measurement Boundary Conditions	8
3.2	Background Concentration ($c_{b,i}$)	8
3.3	Measurement Strategy	9
3.4	Adding Tracer Gas	12
3.5	Taking Air Samples	12
4	Analysis of Test Results	13
4.1	Start.....	13
4.2	Influence of Numerical Integration and of Data Density	13
4.3	Extrapolation of Concentration Gradient to Determine $\mu_i^{(m)}$	14
4.4	Choosing the Reference Value: τ_e or τ_n	18
4.5	Pulse Method	18
5	Problems in Field Measurements.....	19
5.1	Recirculation Air	19
5.2	In- and Exfiltration.....	19
6	Instrumentation and Test Setup	20
7	Results	24
7.1	Ceiling Twist Diffusers.....	25
7.2	Slots.....	30
7.3	Floor Twist Diffusers	34
7.4	Displacement Ventilation (DV)	38
8	Conclusion.....	44
9	Terminology	45
10	References	46

1 Introduction

The purpose of a room ventilation system is to provide adequate thermal temperatures for the occupant's comfort. Furthermore, the ventilation should provide sufficient fresh air to occupants in the occupant area and avoid emitted substances (pollutants) entering the occupant zone and/or remaining within this zone for too long.

In room ventilation systems with nearly ideal mixed room air conditions it does not involve any particular issues in assessing the quality of the system because it is solely determined by the air-exchange rate. Quantification of improvement and quality, however, is more difficult for other ventilation systems, which are being introduced nowadays.

With the tracer gas measurement technology an adequate evaluation parameter can be determined. Two evaluation parameters are known: On the one hand the air change effectiveness, i.e. characterization of the local and global air-exchange and the distribution of supply air respectively; on the other hand the ventilation, or pollutant removal, efficiency, which is characterized by the attenuation, allocation and extraction of harmful gases in the room.

Since the beginning of the 1980's research work in this field was done mainly in the Scandinavian countries. The most proposals for new benchmarks and methods are from researchers in these countries. A comparative and methodic analysis including analysis of the reliability of the measurement procedure has not been done so far.

With this background the task of this work is to develop a tracer gas method and evaluation method to determine the air change effectiveness and the ventilation efficiency in mechanically ventilated rooms. The reliability and suitability for practical use of the method is proved at measurements in the laboratory. Four different realistic systems are verified: two ventilation systems with inlet openings on floor level and exhaust at ceiling level (displacement ventilation and floor twist diffusers), and two systems with both inlets and exhausts at ceiling level (ceiling twist and slot diffusers).

Designing and constructing the measurement facility, as well as the programming of the computer analysis software, turned out to be more difficult than assumed at the beginning. In the limited period of two years the research on the ventilation efficiency was confined to its basic analysis. The analysis of the air change effectiveness was completed successfully. The results are presented in this paper.

2 Principles for Determining Air Change Effectiveness

The air change effectiveness is described with the term "age of the air." The local "age of the air," τ_p , ($p=point$) is a statistical value and a time based measure describing how long air molecules need on average to travel from the entry point into the room to a particular point p in the room (see Figure 1). The shorter this time the better is the air exchange at this particular point p . Arithmetic averaging of all these local ages of the air τ_p result in the average age of the air of the room $\langle \tau \rangle$. This value characterizes the effectiveness of the air-exchange in the entire room as it is addressed in the supply air volume as well as in the performance of its distribution within the room.

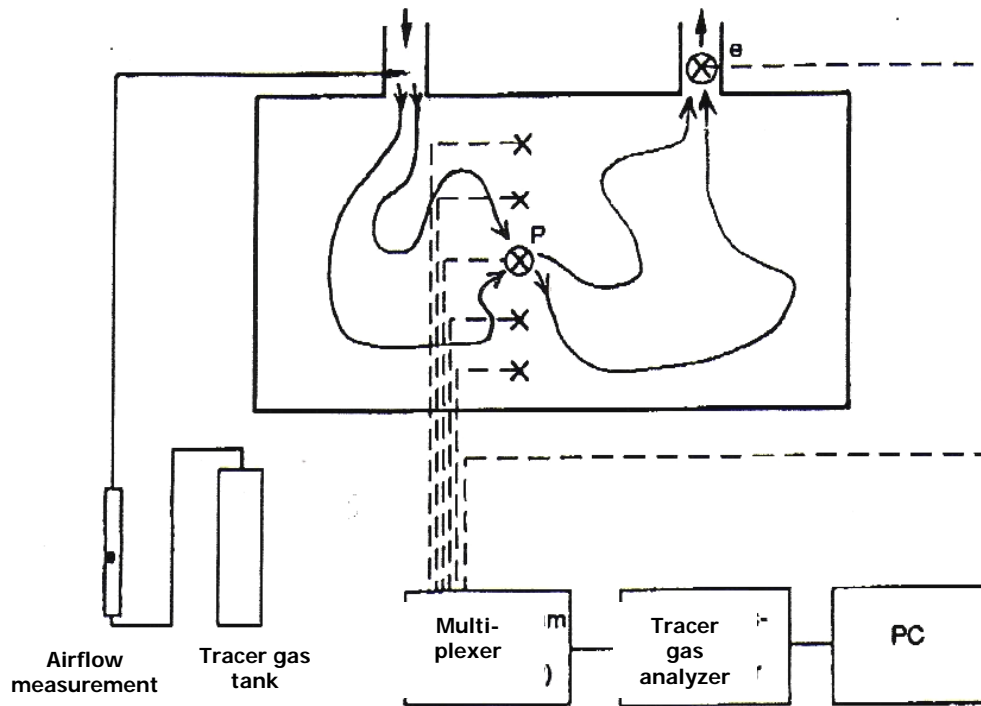


Figure 1. Flow paths of air molecules to a point p in the room and to the exhaust duct e ("age of air" concept) and associated measuring setup

As a reference value for the two values τ_p and $\langle \tau \rangle$ the local "age of the air" within the exhaust channel τ_e is used. If there is no in- or exfiltration in the room, this value is equal to the nominal time constant τ_n and the reciprocal of the air-exchange n ($\tau_e = \tau_n = 1/n$). To characterize the air change effectiveness, the so called local air-exchange index ε_p [-] ($0 < \varepsilon_p < \infty$) and the so called global air-exchange index ε [-] ($0 < \varepsilon < \infty$) are derived:

$$\varepsilon_p = \frac{\tau_e}{\tau_p} \text{ and } \varepsilon = \frac{\tau_e}{\langle \tau \rangle} \quad \text{Equation 1}$$

For both parameters high values are aspired. Reference is the ideal mixed ventilation with $\varepsilon_p = \varepsilon = 1$.

To determine the age of air the supply air is marked with a tracer gas. The resulting, time-dependant concentration gradient at selected locations in the room is recorded. A pump system takes air samples to a tracer gas analyzer, which is controlled through a computer. The following three types of measurements can be used: The step-up method, the step-down method and the pulse method.

- In the step-up method, tracer gas is injected at a constant rate and known concentration (c_s) at the supply duct beginning at the time $t=0$. At the beginning of the test sequence the test room must be free of tracer gas. The tracer gas concentration in the room rises starting with the respective background concentration $c_{b,i}$ (b=background) up to the end concentration $\bar{c}_i(\infty)$.
- In the step-down method, the tracer gas injection to the supply air is stopped at the time $t=0$. The tracer gas concentration in the room must be known shortly before this time $t=0$.
- In the pulse method, a short input pulse of tracer gas at the time $t=0$ takes place. A homogeneous tracer gas mixing with supply air is necessary. The concentration increases from $c_{b,i}$ up to a maximum local value and decreases again to $c_{b,i}$.

To designate the individual ages of air, the so called moments $\mu_i^{(m)} [s^{m+1}] m^{\text{th}}$ order ($0 \leq m \leq 2$) of the time- and dimensionless tracer gas concentration change $c_i^*(t)$ must be calculated:

$$\mu_i^{(m)} = \int_0^{\infty} t^m c_i^*(t) dt \quad \text{Equation 2}$$

In this equation the index i stands for the sample point in the exhaust collecting channel e or for the point of measurement p in the room.

The different age of air values which were calculated using the moments are listed in Table 1 depending on the measurement method. The dimensionless concentration allocations c are shown as well.

Table 1: Determination of τ_p , τ_e , $\langle \tau \rangle$ and $c_i^*(t)$

Method	τ_p	τ_e	$\langle \tau \rangle$	$c_i^*(t)$

Step up	$\mu_p^{(0)}$	$\mu_e^{(0)}$	$\frac{\mu_e^{(1)}}{\mu_e^{(0)}}$	$1 - \frac{c_i(t) - c_{b,i}}{\bar{c}_i(\infty) - c_{b,i}}$
Step down	$\mu_p^{(0)}$	$\mu_e^{(0)}$	$\frac{\mu_e^{(1)}}{\mu_e^{(0)}}$	$\frac{c_i(t) - c_{b,i}}{\bar{c}_i(0) - c_{b,i}}$
Pulse	$\frac{\mu_p^{(1)}}{\mu_p^{(0)}}$	$\frac{\mu_e^{(1)}}{\mu_e^{(0)}}$	$\frac{\mu_e^{(2)}}{2\mu_e^{(1)}}$	$\frac{c_i(t) - c_{b,i}}{c_{ref}}$

$c_i^*(t)$...normalized concentration distribution at point i (in Room $i=p$, in exhaust duct $i=e$)
$c_i(t)$...measured concentration distribution at point i
$c_{b,i}$...background concentration at point i
$\bar{c}_i(\infty)$...average end concentration for $t \rightarrow \infty$ at point i
$\bar{c}_i(0)$...average start concentration at time $t=0$ at point i
c_{ref}	...any reference concentration (e.g. maximum concentration in the supply air)

If the test room does not have a central exhaust channel but uses a hung ceiling or a number of exhaust slots, τ_e and $\langle \tau \rangle$ can be derived from the weighted flow rate at each individual exhaust grille.

Because of the limited measuring period $0 <= t <= t'$, the concentration distribution $c_i^*(t)$ must be extrapolated towards infinity for the calculation of the moments $\mu_i^{(m)''}$ and $\mu_i^{(m)}$. The following integrals have to be calculated:

$$\mu_i^{(m)} = \mu_i^{(m)'} + \mu_i^{(m)''} = \int_0^{t'} t^m c_i^*(t) dt + \int_0^{\infty} t^m c_i^{*''}(t) dt \quad \text{Equation 3}$$

The moment $\mu_i^{(m)'}$ follows from the normal measured distribution $c_i^*(t)$. The residue $\mu_i^{(m)''}$ follows the extrapolated gradient $c_i^{*''}(t)$. For $t' \leq t < \infty$, $c_i^*(t)$ can be derived with $c_i^{*''}(t)$ given in this equation:

$$\ln(c_i^{*''}(t)) = \ln(c_i^*(t)) \Big|_{t' < t < \infty} = a_i(t') - \lambda_i(t')t \quad \text{Equation 4}$$

Using the equation above, $\mu_i^{(m)''}$ can be calculated from Table 2:

Table 2: Calculation of residues $\mu_i^{(m)''}$ of the moments $\mu_i^{(m)}$

m	0	1	2
$\mu_i^{(m)''}$	$-\frac{c_i^*(t')}{\lambda_i(t')}$	$-\frac{c_i^*(t')}{\lambda_i(t')} \left(t' - \frac{1}{\lambda_i(t')} \right)$	$-\frac{c_i^*(t')}{\lambda_i(t')} \left((t')^2 - \frac{2t}{\lambda_i(t')} + \frac{2}{(\lambda_i(t'))^2} \right)$

$c_i^*(t')$ is the last, i.e. at time $t=t'$, measured concentration value and $\lambda_i(t')$ is the degree of the exponent decay at time $t=t'$. The value of $\lambda_i(t')$ does not depend on the type of measurement method (step up, step down or pulse).

3 Realization of and Compliance with Measurement Boundary Conditions

The described methods to define the air change effectiveness are simple in their theoretical substructures. There are some problems in the practice, especially in field measurements, caused by maintaining complicated measurement boundary conditions. Extensive knowledge about ventilation strategies and experimental strategies is essential to achieve reliable results. Literature provides only a small amount of information in this field.

3.1 General Measurement Boundary Conditions

The local value of the age of air can be measured exclusively by recording cyclic concentration differences of artificial inputs of tracer gas into the supply air channel. This means that especially at low airflows testing may require a couple of hours.

Since the age of air is a relative state which depends on *one* specific room airflow pattern, the resulting values can only be interpreted for this one airflow pattern. Timely stability of the room airflow pattern is therefore a requirement for all of the three measuring methods in order to determine air change effectiveness.

This stability is on the one hand depending on external parameters with direct effects on the airflow pattern. These external parameters are e.g. air and heat fluxes entering or leaving the room, surface temperatures of people, equipment and walls, the behavior of people or other moving equipment etc. If the consistence of these parameters can not be guaranteed, the determination of air change effectiveness is usually not reasonable. Local effects of disruptions are recognizable in the distribution of concentrations. However, the quantitative assessment is difficult because the local ages of air are affected diversely, depending on when the disturbance occurs.

On the other hand, inherent influences exist. These can be recognized as unstable room airflow patterns that may develop even though external parameters are constant over time. An example for this is the falling down and mixing of air stratum. Because of the repeatability of measurements, such disturbances can be eliminated through repeated measurements of the local age of air at the same place (p). Standard deviation allows a judgment of the magnitude.

These problems, which were in fact only discovered during testing, seem to be trivial but are not considered and/or don't get the necessary attention in many publications.

3.2 Background Concentration ($c_{b,i}$)

The background concentration $c_{b,i}$ is affected by several factors: The self noise of the gas analysis equipment and the fact that the tracer gas may be part of the naturally occurring gases of the room air (e.g., N_2O).

Local differences of the background concentration in the room occur whenever infiltrated air penetrates into supply or exhaust air ducts *and* whenever it shows a different concentration from the one of the supply duct. These local differences, as well as the background concentration itself, have no negative influences on the measured results, as long as they are constant during the duration of measurement and are also considered during the analysis (refer to Table 1). The same is true for local differences of the end and starting concentration $\bar{c}_i(\infty)$ and $\bar{c}_i(0)$.

These conditions mainly occur in field measurements. At laboratory measurements the following measures help to maintain the background concentration $c_{b,i}$, as well as the local maximum concentrations $\bar{c}_i(\infty)$ and $\bar{c}_i(0)$, constant: a) the room is pressurized with respect to maintaining an exfiltration rate of less than 3%; b) There must not be a connection between exhaust and supply duct (i.e., recirculating air operation).

3.3 Measurement Strategy

Because of unreliable results of the "Pulse Method," the following comments are referred exclusively to the "Step-down" and "Step-up" methods.

Experiments suggest that a cyclical sequence of "Step-down" and "Step-up" experiments is the most reasonable measuring strategy. The use of fans in the room to get a homogeneous initial concentration allocation for the "Step-down" experiment is neither necessary nor practical, because of the following reason.

Particular values of local age of airs are primarily determined through the local gradient of concentration directly after the start of the measurement (i.e. through changes during $0 \leq t \leq 0.5\tau_n$). In order to assure reproducibility of the local age of air, exactly defined conditions at the beginning of each measurement are indispensable. This means, that a step-up and a step-down test, respectively, can only be started after all time-gradients of the concentration are nonexistent in the exhaust duct (refer to Figure 3). Because of the fact that fans produce an artificial and incidental flow pattern, reproducibility of starting conditions can not be assured. Even more severe is the resulting error. After switching off the fans, the actual air pattern which is to be studied needs to generate itself first. This process, however, falls into the above mentioned time frame.

While choosing a tracer gas quantity with a maximum concentration $\bar{c}_i(\infty)$ and $\bar{c}_i(0)$ respectively, with a 500 times greater dose than the detection limit c_d of the gas analyzer, the duration of measurement for an air distribution system with $\varepsilon = 1$ is approximately $\Delta t_{total} = 7\tau_n$ for the step-up method and about $\Delta t_{total} = 8.5\tau_n$ for the step-down method (refer to Figure 2). For systems with ventilation efficiencies of $\varepsilon \neq 1$, Δt_{total} is more or less for both systems at about $5.5(1 - \varepsilon)\tau_n$.

Furthermore, it turned out to make sense to measure the local age of air twice for the same spot. First, the step-up method is to be applied and immediately afterwards the

step-down method. Since both methods turned out to be reasonable, the timely stability of the local air-exchange at the point ρ and the stability of the air flow pattern of the room, respectively, can be verified.

To designate the repeatability of the measured age of air, the absolute standard deviation $s_n = \sqrt{\sum_{n=1}^k (\tau_{i,k} - \bar{\tau}_i)^2 / (n-1)}$ is derived for individual ages. For the average room age $\langle \tau \rangle$, a value of $s_{10...16} \leq 0.025\tau_e$ and for the local age inside the exhaust duct, τ_e , a value of $s_{10...16} \leq 0.010\tau_n$ turned out. Basis of both values is $2 \times (5...8)$ measuring loops at constant boundary conditions of the ventilation system.

Repeatability of the individual local ages usually was above $s_2 = 0.025\tau_e$: this was the case for overhead systems with 95% probability, for underfloor systems using swirl diffusers with 75% probability and for displacement ventilation systems with 60% probability. Low repeatability turned out for test conditions that had unstable thermal recirculation. Within the stable low airflow zones of the displacement ventilation system, in which relatively low local ages from $0.2...0.5\tau_e$ were measured, repeatability was extraordinarily good. Standard deviation was about $s_2 \approx 0.01...0.05\tau_e$. For only 1% of the total number of measurements of the local age of air, which were conducted twice, s_2 was greater than $0.1\tau_e$.

However, we can not draw the conclusion out of this high reproducibility, that one single measurement is enough. High repeatability can only be achieved, as mentioned earlier, when boundary conditions are carefully realized and the measurement system works immaculately. Measuring two times allows to show deviations thereof. This is particularly important in field measurements in which boundary conditions can not be defined accurately.

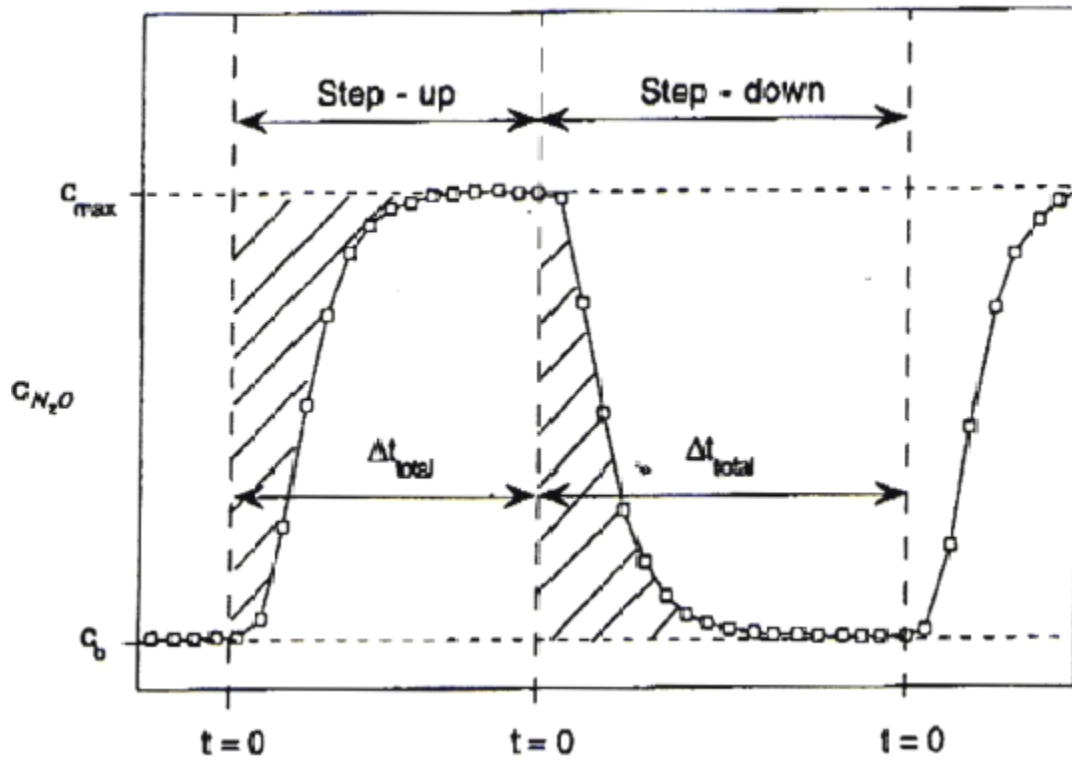


Figure 2: Cyclic sequence of "Step-up" and "Step-down" experiments

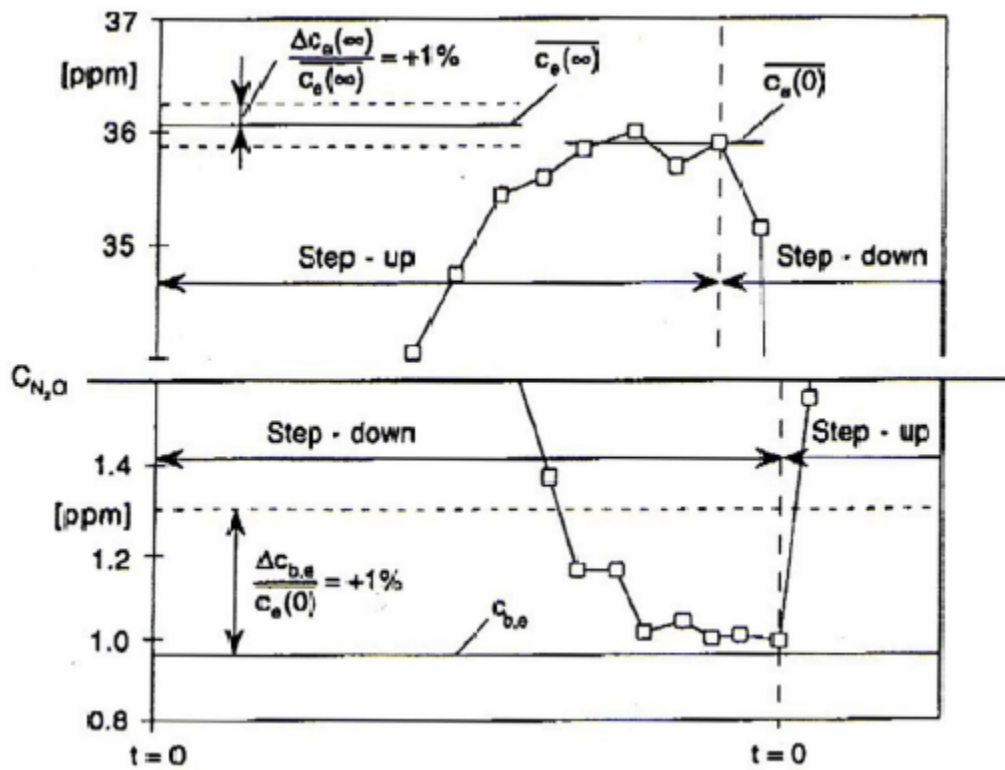


Figure 3: Magnification of concentration distribution of Figure 2

3.4 Adding Tracer Gas

The step up method requires that the entire mechanically delivered air at the inlet within the timeframe $0 \leq t < \infty$ is marked with a time constant and homogeneous tracer gas concentration. Such a homogeneous mixture can be achieved by using straight, ring-shaped or cross-shaped hose pieces for dosing the tracer gas into the supply channel. These hoses, made from polyethylene or polyamide, have to be perforated with a thin needle to achieve a homogeneous escape of air over the entire length of the hose and over the entire cross section of the supply channel, respectively. The more such devices are used, the shorter can the mixing routes between the place of dosage and the diffuser be.

3.5 Taking Air Samples

Shortly after the exhaust grille, inhomogeneous tracer gas concentrations usually occur. If it is not possible to take measurements further down stream, a median concentration value and concentration distribution, respectively, of the particular exhaust grille can be determined. This can be done by using the same hose apparatus as for dosing.

Values of local indices ε_p in the room differ even at very short distances of only a couple centimeters (e.g. within and outside the upward stream of a warm body). Due to this reason, *only* point measurements at each interesting place p in the room should be obtained.

In several publications an average air change rate in the occupied zone is determined with measurements at many arbitrarily chosen points. The ε_p values are either calculated arithmetically or these points of measurement are merged together in one air sample, in order to obtain *one* concentration distribution that is representative for the entire occupied zone. The allegation of such an average air change rate is not reasonable because of a dependency on the value at the chosen points in the room and of the number of measured points. Rather a determination between local indices ε_p and the global index ε is practical to evaluate the air change rate in the occupied zone. This hypothesis is proven later in the experiments.

4 Analysis of Test Results

4.1 Start

The applied measurement system controlled the time when the air probe is taken. Start time for the analysis is $t=0$ (time where tracer air penetrates the room).

The flow rate of the air conditioning system and the tracer gas pumps are limited. Finite durations are needed to a) transport the tracer gas from the bottle to the injection point in the inlet channel, b) from the injection point to the inlet and c) from the measurement points through the tubes to the gas analyzing monitor.

All individual time delays have to be added to the time, where the tracer gas is injected into the supply air channel (step-up method) or where the tracer gas is stopped (step-down method). At the negligence of a time delay of $x\tau_n$ all moments $\mu_i^{(m)}$ ($0 \leq m \leq 2$) are systematically defined $x(\tau_n)^{m+1}$ too high.

The delay time is either determined by the sum of the volume flow based on the delay volume in the individual tubes and duct sections or directly by adding smoke at the place of dosage.

4.2 Influence of Numerical Integration and of Data Density

Local concentration distributions are measured simultaneously at several points using *one* gas analyzer. The distributions are not continuous but discrete. These values have to be integrated for the moments $\mu_i^{(m)}$. Several numerical integration methods are assessed to get the smallest reliable data rate. This was done by artificially created concentration gradients added by a random mistake. The common used "trapeze method" needs a data density of at least $N_{min} = 5 \text{ values} / \tau_n$. Considering the stability and the accuracy, interpolation polynomials of second or fourth order are considered to be the best. Both are independent from the air conditioning system with a data rate of $N_{min} = 3 \text{ values} / \tau_n$.

The maximum number of points of measurement $N_{s,max}$ ($s = \text{sample}$) at a step-up and a step-down test, respectively, is derived from

$$N_{s,max} = \frac{1}{N_{min} \Delta t_{ana}} \quad \text{Equation 5}$$

For example, if the time of analysis of the gas analyzer for a probe Δt_{ana} is 40 seconds, the air exchange rate is 5 ($\tau_n = 1/n = 12 \text{ min}$) and an interpolation polynomial of second or fourth order is used ($N_{min} = 3 \text{ values} / \tau_n$), the age of air can be measured on

$N_{s,max} = 6$ places simultaneously, i.e. on 5 places inside the room and on one reference point inside the exhaust duct.

4.3 Extrapolation of Concentration Gradient to Determine $\mu_i^{(m)}$

The extrapolation method is based on the so called NORDTEST method. The principle of the CLRM (continuous linear regression method) is as follows (refer to Figure 4 and Figure 5):

- during the entire measurement period $0 \leq t < \infty$ a linear regression of the latest measured N_{fit} logarithmic concentration value $ln c_i(t)$ is conducted after each new measured concentration value according to Equation 4
- at a constant number of N_{fit} an actual value of λ_i is given for all time steps t
- as these values λ_i are applied over time, an asymptotic rising or falling gradient can be found which approaches a constant end value $\lambda_i(t)'$
- the number of values N_{fit} that go into the linear regression are used to determine both how smooth and fast the individual gradients $\lambda_i(N_{fit})$ approach the uniform end value $\lambda_i(t)'$. This is important whenever scattered concentration distributions are to be analyzed.

The main advantages of the CLRM method are:

- an additional adjustment of local end concentration is possible for both methods step-down and step up if the local end concentration changed during the measurement period
- extrapolation is possible at any time step $t=t'$
- only the CLRM method allows getting the same reliable results of step-up method and step-down method

Therefore, extrapolation is no longer an uncertainty factor for the entire measurement method.

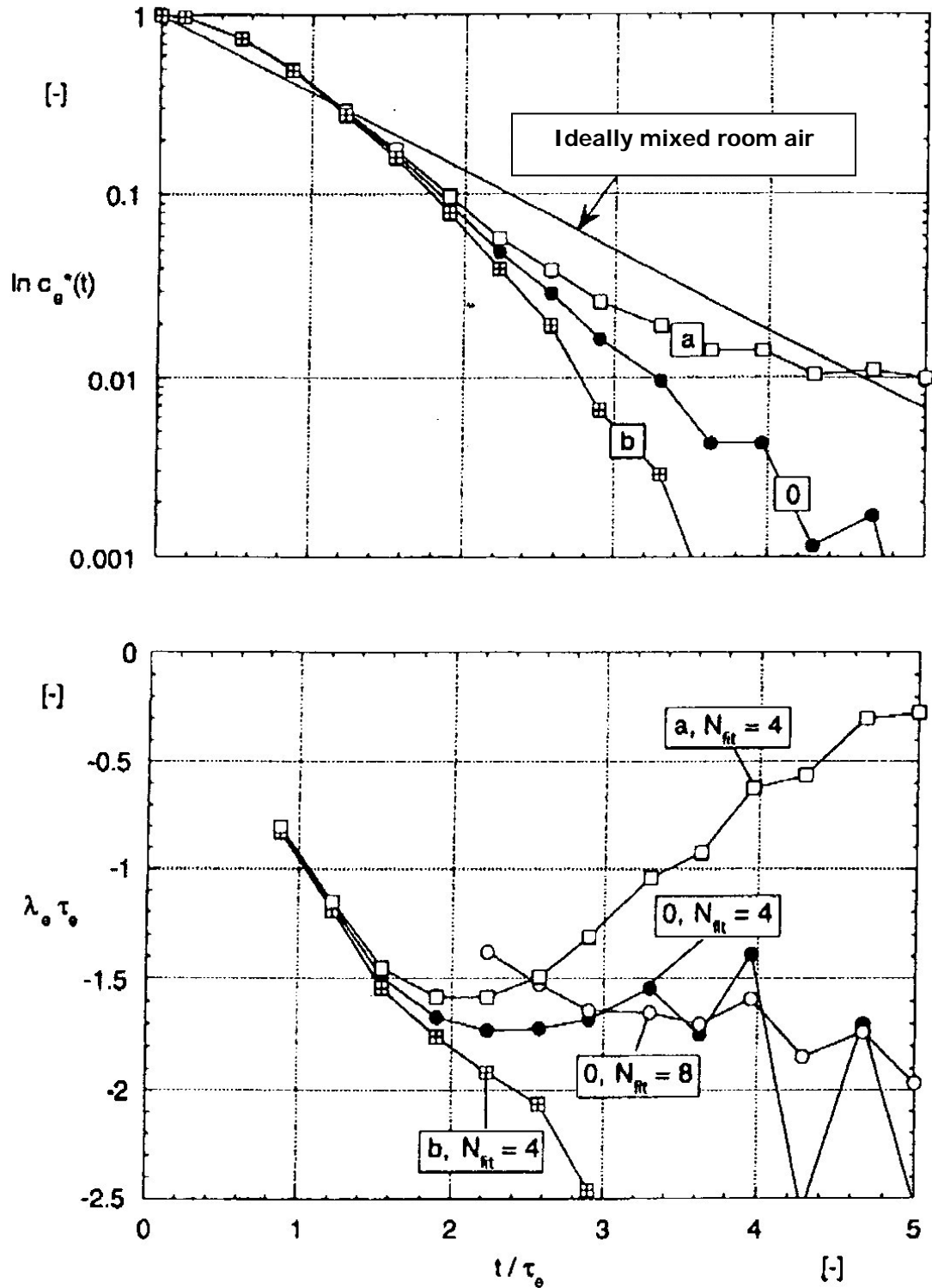


Figure 4: Normalized concentration distribution of the step down test from Figure 2. Influence of background concentration (curve 0: correct assumption of $c_{b,e} = 960$ ppb and $c_e(0) = 35.8$ ppm; curves a and b: $\Delta c_{b,e}/c_e(0) = \pm 1\% \rightarrow \Delta \tau_e / \tau_e = \pm 2.5\%$ and

$\Delta \langle \tau \rangle / \langle \tau \rangle = \pm 4\%$ in these distributions; upper graph) and relevant distributions of λ_e (lower graph).

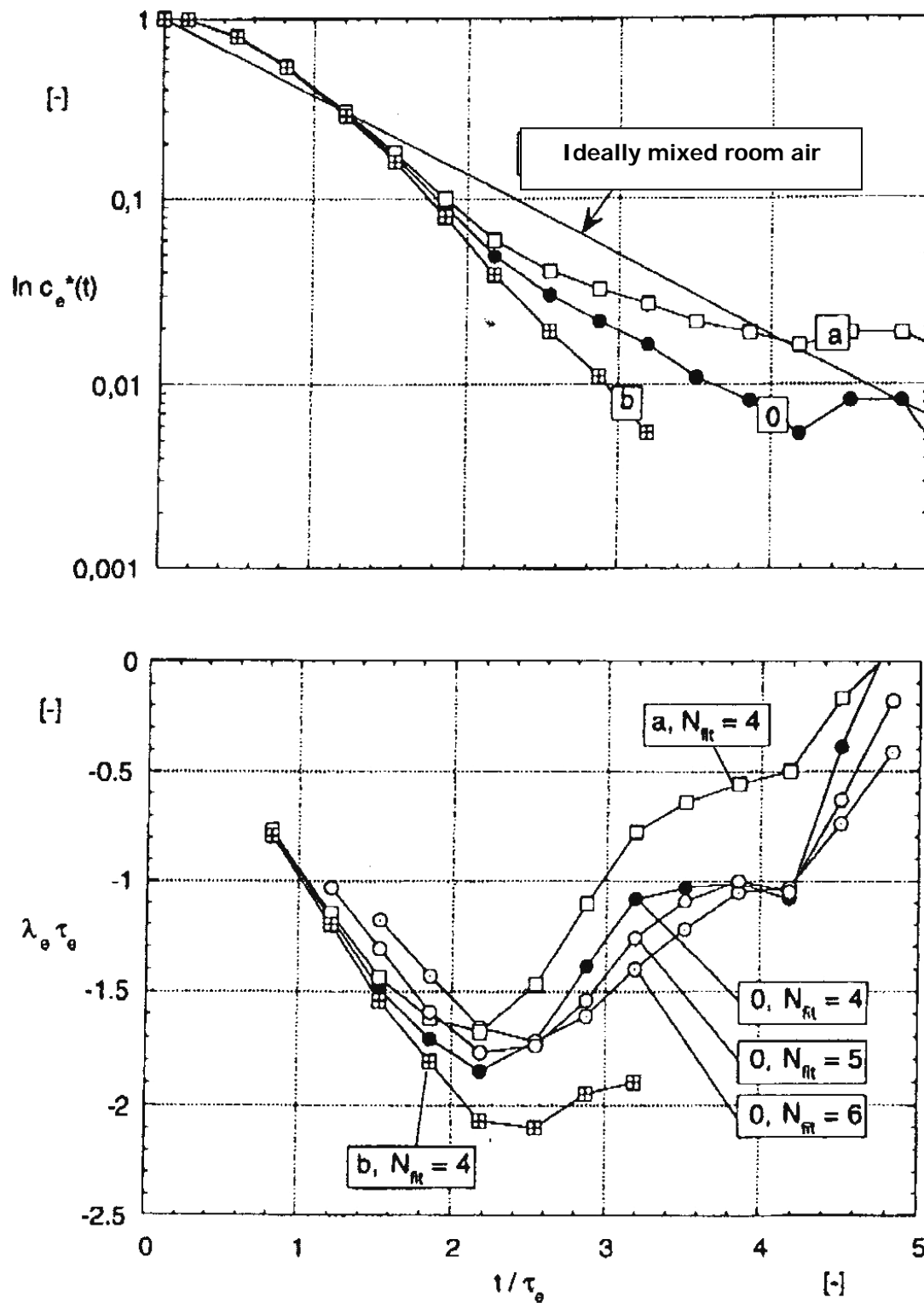


Figure 5: Normalized concentration distribution of the step up test from Figure 2. Influence of background concentration (curve 0: correct assumption of $c_{b,e} = 960$ ppb and $c_e(0) = 36.2$ ppm; curves a and b: $\Delta c_e(\infty)/c_e(\infty) = \pm 1\% \rightarrow \Delta \tau_e / \tau_e = \pm 2.5\%$ and

$\Delta \langle \tau \rangle / \langle \tau \rangle = \pm 4\%$ in these distributions; upper graph) and relevant distributions of λ_e (lower graph).

4.4 Choosing the Reference Value: τ_e or τ_n

During the absence of in- or exfiltration, τ_e equals τ_n . However, the local age measured in the return air channel τ_e is *always* to be preferred as the reference value for the individually measured local age of air values.

To get an agreement between the values of τ_e and τ_n the nominal time constant τ_n (or an air exchange rate n) is not to be interpreted in the sense of a specific air exchange rate. Because of the temperature and pressure differences between inlet air, room air and exhaust air the following equation is to be considered:

$$\tau_n = \frac{M_r}{\dot{M}_s} = \frac{M_r}{\dot{M}_e}$$

In this equation M_r is the mass of the air inside the room that is to be exchanged, \dot{M}_s and \dot{M}_e are the mass flow rates in the supply and exhaust ducts, respectively.

4.5 Pulse Method

The pulse method has the following disadvantages compared to the Step-up and the Step-down methods:

- At the beginning of the measurements the gradient as well as the curvature of the $c(t)$ plots are very high. A major problem is the determination of the time of zero order.
- The signal-flush ratio of the plot is low because of the limited injection time and because of the low tracer gas concentration.
- Short time local instability of the room ventilation
- The time of measurement for the concentration is shortly after the interruption of the tracer gas injections (pulse). A typical air movement is often not given to this time.

Due to these reasons, the pulse method does not qualify for determining air change effectiveness.

5 Problems in Field Measurements

Different operation methods occur to define the ventilation efficiency at field measurements compared to the laboratory measurements. It is important to mention the recirculating air operation because of the use of VAV controls.

5.1 Recirculation Air

A constant tracer gas input is necessary in both the Step-down and the Step-up method during the entire test duration $0 \leq t \leq \infty$. This boundary condition can not be fulfilled in recirculating air operation tests.

With the help of the multi zone model CONTAM86 the recirculation air operation is tested with small and medium sized ventilation systems (which means small recirculation volumes compared to the volume of the room), as well as large systems (with large recirculation volumes). A practical procedure to test the dynamic behavior of the room air or the ventilation system is not found. The recirculation air operation behaves like a permanent internal air circulation in the room at small recirculation volumes. Local indices X_p are usually close to 1.

Following these results the recirculation air operation is to be limited to a tenth of a percent. Otherwise the Step-down method is not applicable. The Step-up method is applicable in the case that the tracer gas input is controlled (to get a constant air input concentration).

5.2 In- and Exfiltration

During the appearance of in- or exfiltration the activity of the test will not change. The cyclic order of the Step-up and Step-down method is applicable.

A two-zone model is used to find this approach. The mechanical air volume flow of the inlet is larger than the outlet (high pressure in room). The concentration $c(\infty)$ or $c(0)$ is equal in the entire room. Step-up as well Step-down methods result in the same effect. The two indices according to Equation 1 define the local and global air change rate of the mechanical exhausted air (part of the inlet air which is measured at the particular point in the exhaust channel).

Because of infiltration the mechanical exhaust airflow is larger than the inlet air flow (low pressure in room).

A consideration of the infiltration part is possible because of the allegation of the part of induced local air change rates based on the entire local and global air change rate (mechanical plus infiltrated part).

It is clear that the in- and exfiltration has no influence on the measurements compared to the common approach. For a complete evaluation of the local and global air change rate the additional knowledge of all air flows in or out of the room is necessary.

6 Instrumentation and Test Setup

Inside a test chamber (12m by 6m by 4m high), a model room was built (6m by 4m and 2.8m high) and setup for investigations for displacement ventilation, floor twist, ceiling twist and slot diffusers (Figure 6 and Figure 7). The number and size of diffusers could be changed according to the rate of air flow. Exhaust air was removed through 4 symmetrically installed lighting fixtures. The model room was insulated with 50mm thick Styrofoam panels. In addition, the surrounding of the model room (i.e., the test chamber in which the model room was built) was temperature controlled in order to create nearly adiabatic test conditions.

For determining supply and return air flows two orifice plates were installed according to DIN 1952 standard. Wall temperatures were measured using thermocouples on 10 different locations throughout the room. Space temperature was measured with two mobile, vertical trees, each equipped with 10 thermocouples.

Testing was conducted using 3 air exchange rates (i.e. 2.5, 5 and 8 per hour) and 3 specific load levels at 20, 40 and 65 W/m² in two parameter variations:

- The first one was carried out with constant internal load of 20 W/m² and fixed arrangements of the heat sources. The objective was to investigate the impact of air exchange rates and the temperature difference between return and supply air temperature, respectively (Table 3 and Figure 8).
- The objective of the second test series was to investigate the impact of arrangement and type of heat sources in the room. When internal loads were increased, air exchange rates were adjusted in order to keep a constant temperature difference between return and supply air temperature of about 8.5K (15°F).

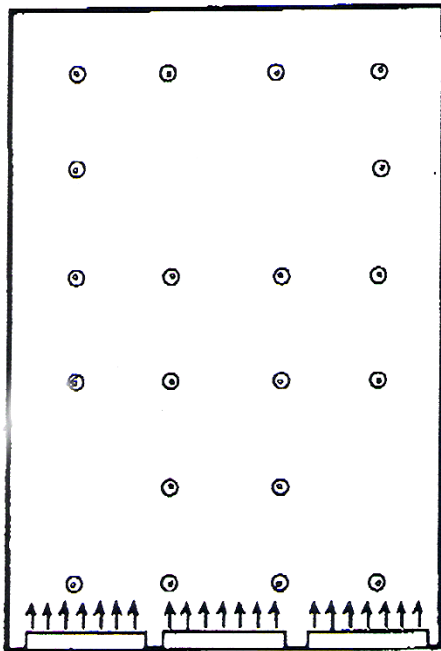


Figure 6: Arrangement of Displacement and Floor Twist Diffusers

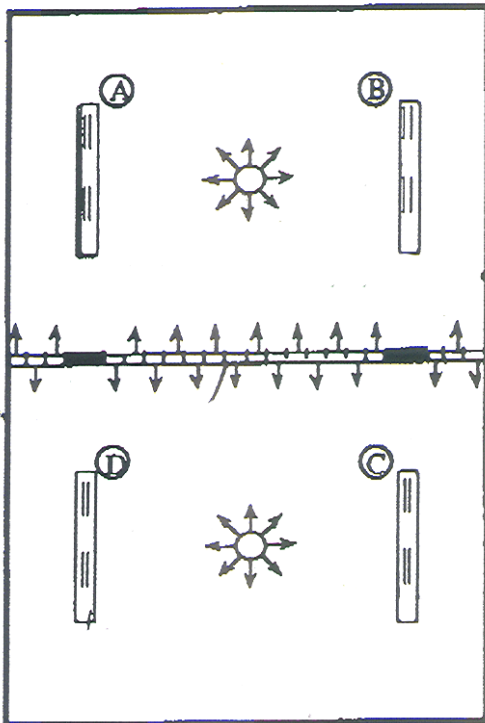


Figure 7: Arrangement of Ceiling Twist and Slot Diffusers and Ventilating Fixtures (A, B, C and D)

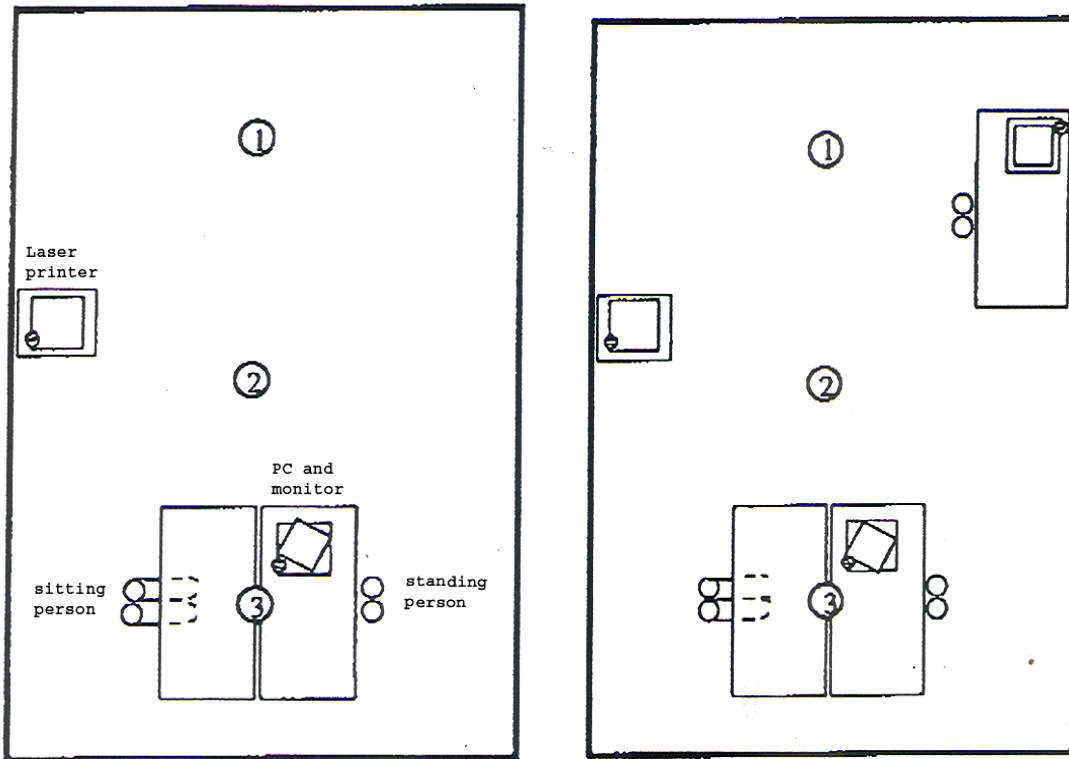


Figure 8: Arrangement of Heat Sources in the Room at $\Delta T = 2.7$ K (left) and $\Delta T = 8.5$ K (right) and position for TC trees (1, 2 and 3)

Table 3: a) Type and Distribution of Heat Loads and b) temperature differences between return and supply air depending on heat load and air exchange rate

Internal Gain	20 W/m ²		40 W/m ²		65 W/m ²	
	Amount	Internal Gain [W]	Amount	Internal Gain [W]	Amount	Internal Gain [W]
a) Distribution						
Manikins	2	200	2	200	3	300
PC + Monitor	1	140	1	140	2	360
Laser Printer	1	60	1	60	1	60
Lighting		80		80		80
Floor Heating				480		740
Total load:		480		960		1540
Point load:		85%		40%		45%
Area load:		15%		60%		55%
b) Air exchange	Temperature difference between return and supply air					
2.5 h ⁻¹	8.5 K					
5 h ⁻¹	4.2 K		8.5 K			
8 h ⁻¹	2.7 K				8.5 K	

For data acquisition, a system provided by Brüel & Kjær was used which turned out to be reliable and free of interferences. The system comes with an IR-gas-monitor Type 1302 and an automated apparatus for proportioning the tracer gas. Furthermore, the system was able to measure air samples at 6 locations in the room.

7 Results

The experimental results for the four air distribution systems can be summarized as follows: The respective systems differ in some parts significantly according to air change effectiveness. All systems showed that, in the first place, the relationship between forced flow and thermal buoyancy-driven flow influences the local air exchange within the room. However, this relationship does not influence the total air exchange. The correlation between forced and buoyancy-driven flow is reflected in the temperature difference between return and supply air temperature. That means that

- the type and arrangement of the heat sources and heat sinks,
- the load ratio between punctual and laminar heat sources, as well as the
- arrangement of supply air inlets and exhaust air grilles play an important role.

The following sections provide a detailed discussion of the results for all 4 air distribution methods. Furthermore, the design case with $n=8h^{-1}$ and a ΔT of 8.5K, respectively, discusses the resulting flow pattern using the local indices ε_p (local air change effectiveness) and the room temperatures at different heights. Selected locally determined values are summarized in Table 4.

Table 4: Selected Local Values of Ventilation Effectiveness and Room Air Temperatures at Design Case

Measurement	Place of Measurement	Ceiling Twist	Ceiling Slot	Floor Twist	DV	
Local value of ventilation effectiveness ε_p [1]	Light fixture A	0.95	0.98	1.03	0.96	
	Light fixture B	1.03	0.98	1.22	1.22	
	Light fixture C	1.05	1.03	1.00	0.94	
	Light fixture D	1.01	1.00	0.88	0.89	
	Section 3					
	Nose of standing manikin	0.95	0.94	1.47	1.22	
	0.3m in front of standing manikin	0.95	0.93	1.13	1.00	
	Nose of sitting manikin	0.97	0.95	2.01	1.68	
	0.3m in front of sitting manikin	0.98	0.95	1.79	1.44	
	Section 1					
	Nose of standing manikin	0.93	0.93	1.87	1.90	
	0.3m in front of standing manikin	0.92	0.93	1.20	1.04	
Air temperature [°C]	Supply	17.1	16.4	18.1	17.6	
	Return	25.6	25	26.7	26.2	
	ΔT	8.5	8.6	8.6	8.6	
	Light fixture A	25.4	24.7	26.9	-	
	Light fixture B	25.9	25.3	27.5	-	
	Light fixture C	24.2	24.3	26.7	-	
	Light fixture D	25	24.4	26.5	-	

7.1 Ceiling Twist Diffusers

The analyzed non-isothermal cases (refer to Table 3) result in small bandwidths of global air change effectiveness ($0.96 < \varepsilon_p < 0.98$). Local indices in the occupied zone of the room (section 2 and 3 in Figure 8) are between $0.89 < \varepsilon_p < 0.97$ with temperature differences less than 0.5K. Visually, the high-inductive diffusers create in the occupied zone – independent of internal load – an almost diffuse flow pattern with mixing character. Therefore, one would expect an effectiveness of around 1. The actual results, however, differ from this value. This is due to two factors, which can not be separated by using the tracer gas method, though. First, the air-exchange between upper and lower zone of the room are not perfect which can be seen in the different exchange indices in both sections. Because air is distributed from top to top, the supply with fresh air in the upper zone of the room is better than below (Figure 9). Second, the distance between supply and return air grilles turned out to be too small, therefore creating short-circuiting of the airflow which lowers the air-exchange indices.

[The points in the following figures refer to global values in air change effectiveness, whereas the points connected with a line refer to local air change effectiveness.]

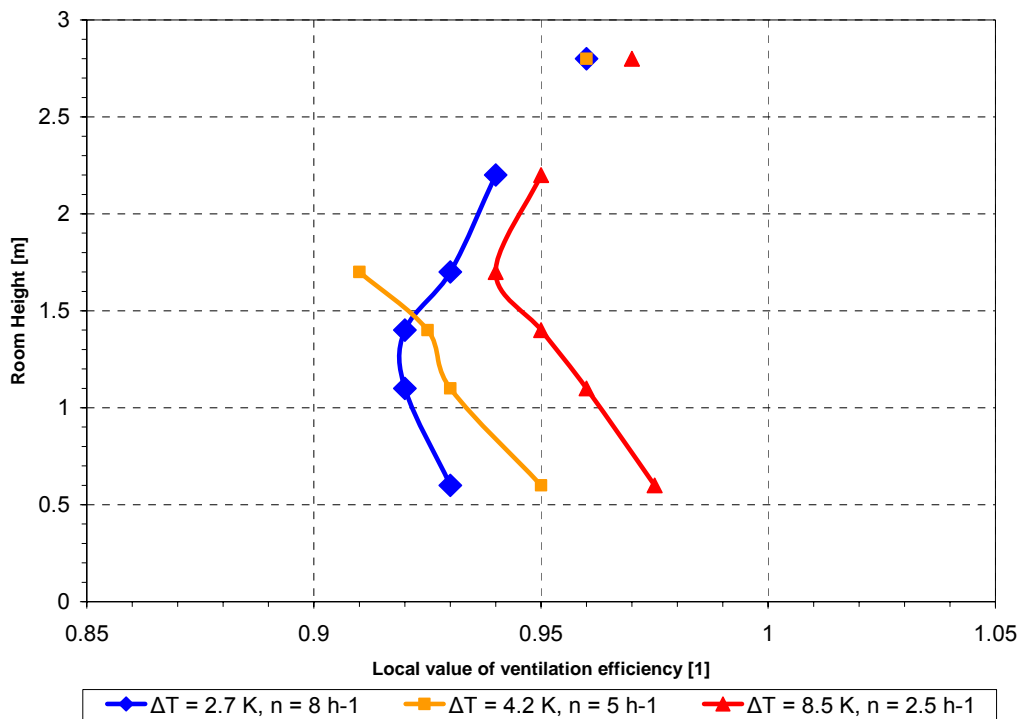


Figure 9: Ceiling Twist Diffusers, Vertical Distribution of Local and Global Air Change Effectiveness at Section 2 as shown in Figure 8 for 20 W/m² Internal Gain

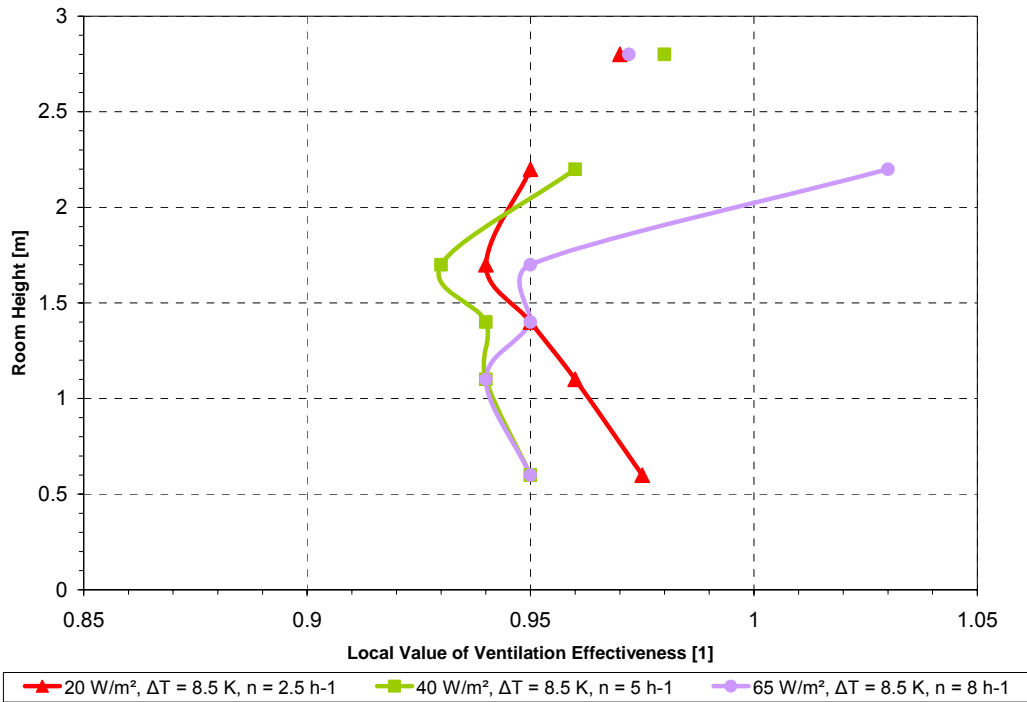


Figure 10: Ceiling Twist Diffusers, Vertical Distribution of Local and Global Air Change Effectiveness at Section 2 as shown in Figure 8 for 20, 40 and 65 W/m² Internal Gain

Moreover, the summarized assessment (presented through the global indices) can be investigated in more detail by looking at the local air change effectiveness. These show secondary structures of the flow pattern. In isothermal conditions (Figure 11) with $n=8$ per hour and the mentioned arrangement of supply and return air grilles the short-circuiting of the air and incomplete air-exchange between top and bottom of the room are most distinctive. Thermal buoyancy effects caused by the heat sources improve the mixing of air in all cases. In addition, buoyancy driven flows reduce direct short-circuiting of the room air on return air grilles located above the heat sources. Accordingly, both indices ϵ_p (local) and ϵ (global) move towards ideal mixing with increased temperature difference between return and supply air temperature.

Due to one-sided arrangement of the heat sources in section 3 (refer to Figure 8), especially at internal gains of 20 and 40 W/m², circulation of room air flow was created throughout the entire room. Supply air was pushed away towards section 1 of the room, which caused an asymmetric distribution of fresh air near the ceiling. This led to the effect that direct short-circuiting was only established in lighting fixtures A and B and that the local ϵ_p at position 1 was about 0.05 higher with air temperatures about 0.5K lower than at position 3. Coupling between air temperature and ϵ_p was found for all cases as shown in Table 3.

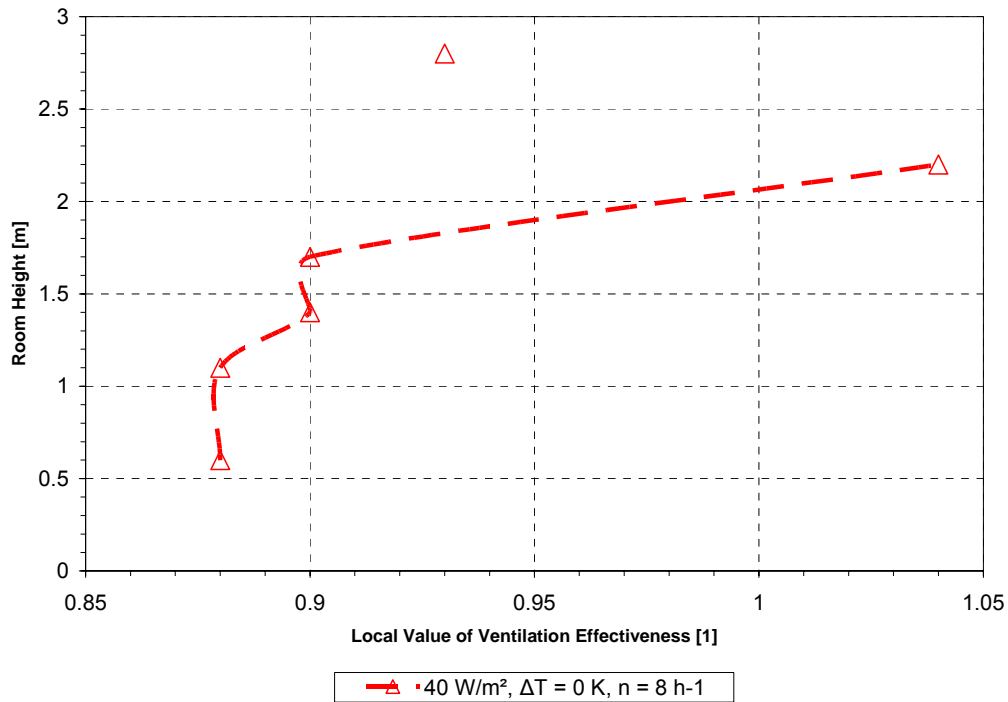


Figure 11: Ceiling Twist Diffusers; Vertical Distribution of Local and Global Air Change Effectiveness at Section 2 as shown in Figure 8 for an Isothermal Case

A detailed review of the design condition (65 W/m^2 , $n=8$ per hour and $\Delta T=8.5\text{K}$) yields the following results. Again, a diffuse flow-pattern can be found which is superimposed by a weak air circulation. Thermal lift was driven by the heat source located below lamp B, which changed the orientation of the circulation of air within the room. Air-exchange in section 3 was now better than in section 1 (Figure 12). This is also reflected in the local indices ϵ_p in the occupied zone and breathing area (Table 4), as well as in the vertical temperature distribution (Figure 13). Measured values for ϵ_p in the light fixtures suggest that short-circuiting occurred in lamp C (lowest ϵ_p and highest temperature). Other measured values are too inconsistent to confirm the relationship between ϵ_p and temperature in the light fixtures for the other load cases.

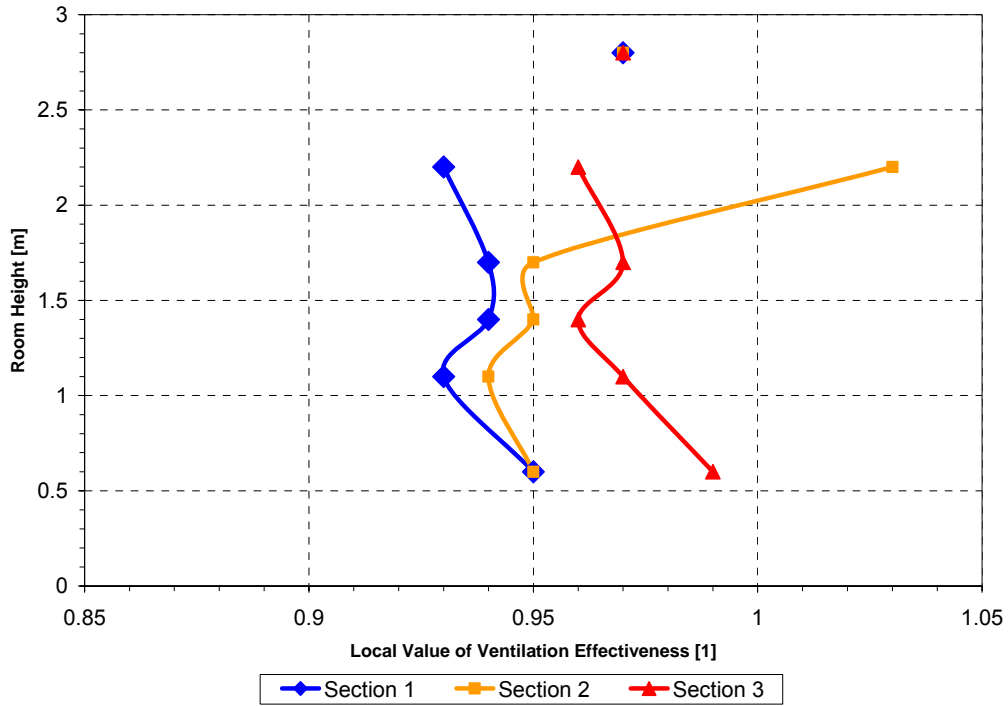


Figure 12: Ceiling Twist Diffusers; Vertical Distribution of Local and Global Air Change Effectiveness at Sections 1, 2 and 3 for the Design Case

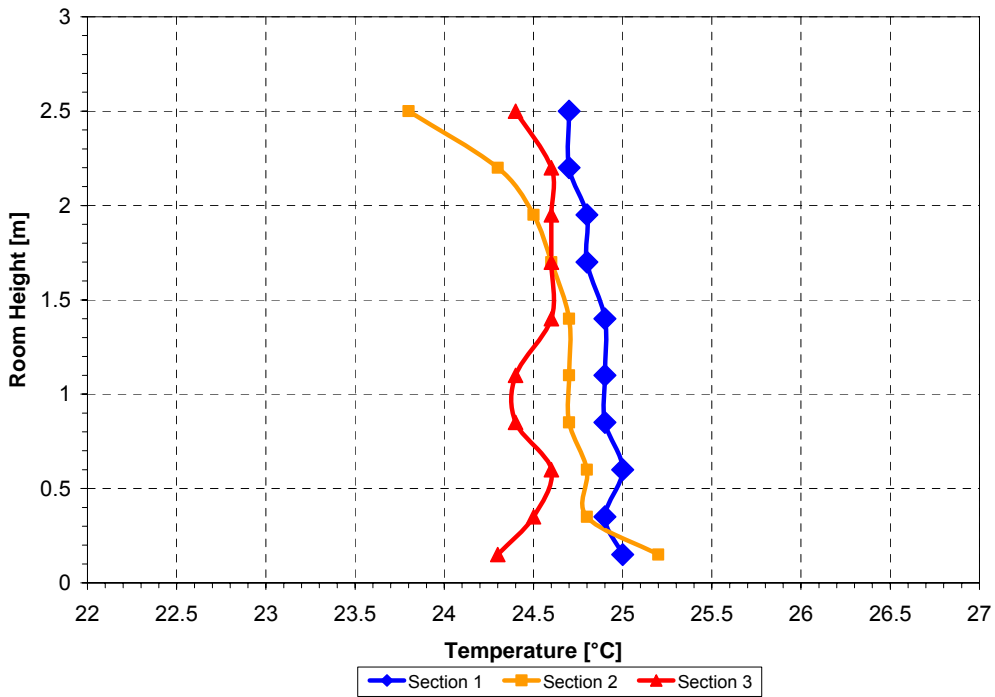


Figure 13: Ceiling Twist Diffusers; Vertical Distribution of Room Air Temperature at Sections 1, 2 and 3 for the Design Case

To clarify the obvious disadvantageous arrangement of supply and return air grilles, two different arrangements are discussed where air is supplied at one part of the room and exhaust air is removed in the other part of the room. This was done at $n=5$ per hour with a $\Delta T=8.5K$. Air was first supplied in section 1 and then in section 3. Success of this approach is shown in Figure 14 and Figure 15. By evaluating the local indices ϵ_p the room airflow pattern can be perceived. There was no short-circuiting of the airflow and also, all parts of the room were completely mixed. In fact, a flow pattern with changing character from the supply air part of the room to return air part of the room was established. This can be verified by the local indices ϵ_p slightly greater than 1 and the lower temperature in the supply air part of the room. In the part of the room where exhaust air was removed, air-exchange was similar to the air-exchange values measured in the return air ducts ($\epsilon_p \approx 1$, highest temperature in the room). Furthermore, the arrangement of the heat sources does not seem to have an impact on the flow pattern primarily driven by the arrangement of the supply air inlet location. If occupants want to recognize the improvement of air quality, they should be placed directly below the diffusers which supply air.

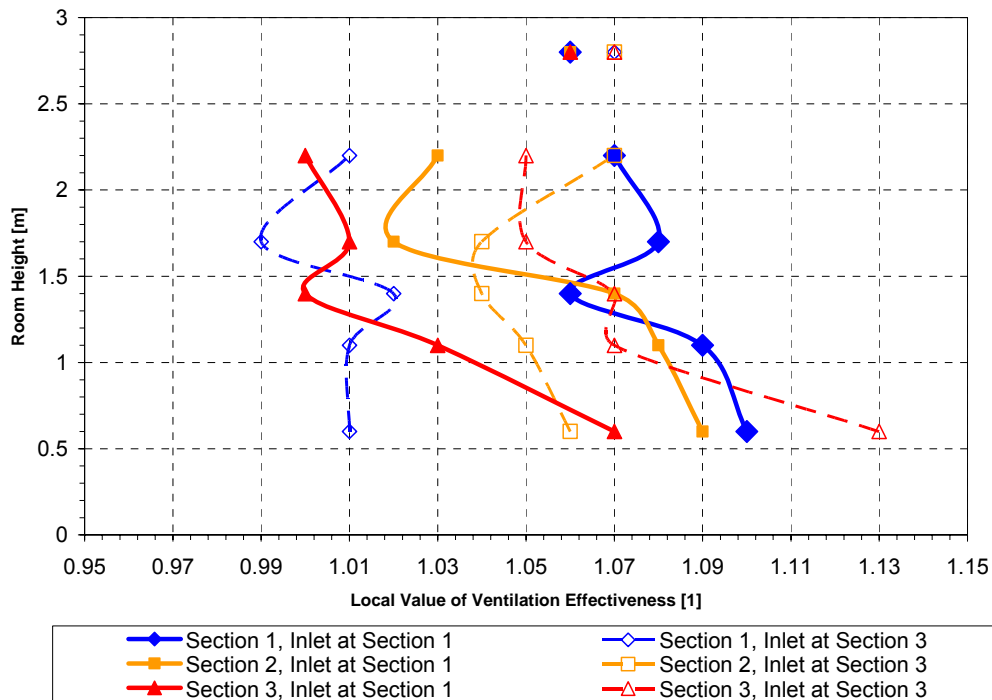


Figure 14: Ceiling Twist Diffusers; Vertical Distribution of Local and Global Air Change Effectiveness at Sections 1, 2 and 3 for $n=8$ per hour and $\Delta T=8.5K$

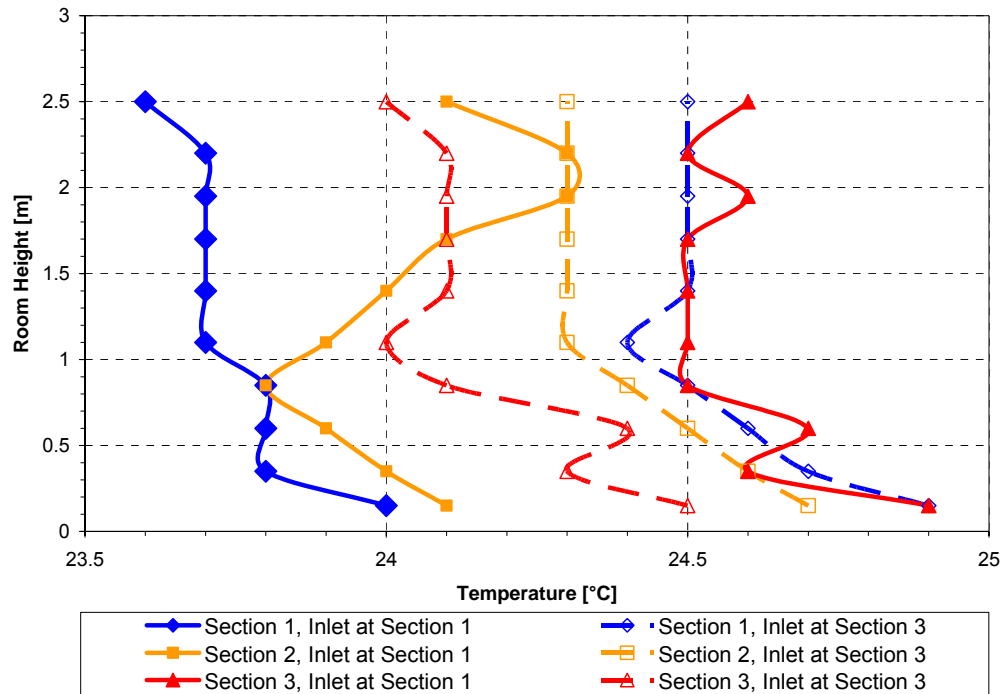


Figure 15: Ceiling Twist Diffusers; Vertical Distribution of Room Air Temperature at Sections 1, 2 and 3 for $n=8$ per hour and $\Delta T=8.5K$

7.2 Slots

The discharge angle of the slots can be adjusted. For the following tests, the angle was chosen to blow the air in two ways and tangential to the ceiling (refer to Figure 7).

For the first test with $n=8$ per hour and $\Delta T=2.7K$ the air entered throughout the whole width of the room. Here, the lowest global value of ϵ (about 0.87, represented by the green line in Figure 16) for the entire testing sequence was found. The fact, that global and local indices were almost the same and that in the light fixtures the indices were 1, short-circuiting was present. Therefore, slots blowing directly at the lighting fixtures were closed with duct tape. The respective slots are marked black in Figure 7. By doing this, the global indices increased to about $\epsilon=0.95$ and the remaining short-circuiting was spread equally between all 4 light fixtures. As illustrated in Figure 16, the local indices were moved parallel towards an ideally mixed system. As a result, direct short-circuiting does not have a negative impact on distribution of fresh air when air distribution systems with mixing characters are used. However, they lead to loss of delivered fresh air. Because of this fact, the slots blowing directly toward the return air fixtures remained closed for the rest of this test series. Independent of the internal heat gain, air-exchange rates were similar. The spectrum of achieved values for global and local effectiveness was within the accuracy of the instrumentation.

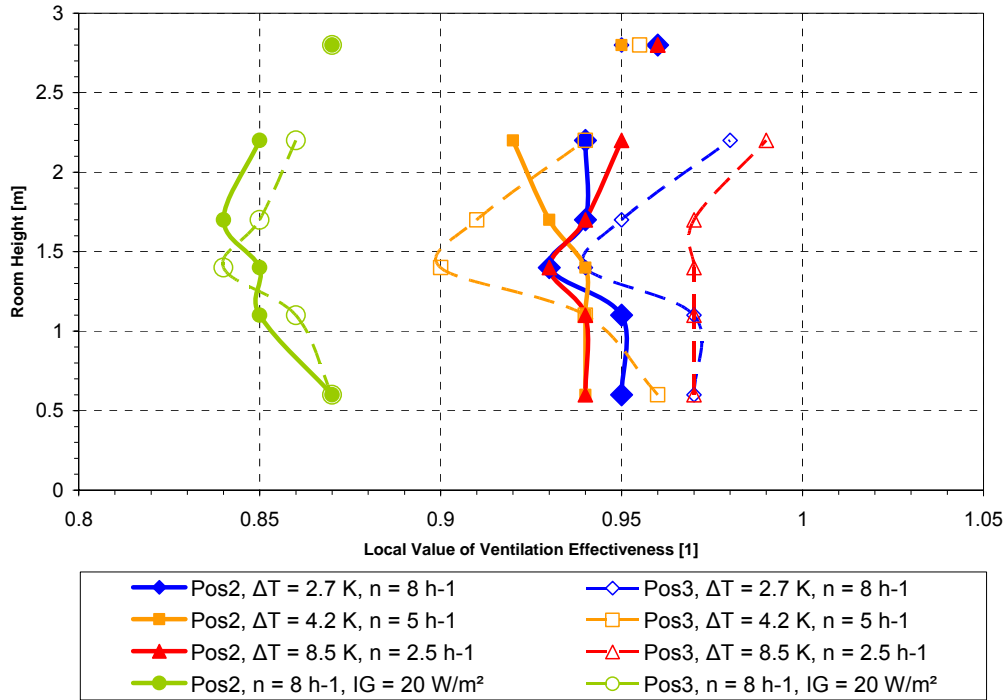


Figure 16: Ceiling Slots; Vertical Distribution of Local and Global Air Change Effectiveness on Position 2 and 3, IG=20 W/m²

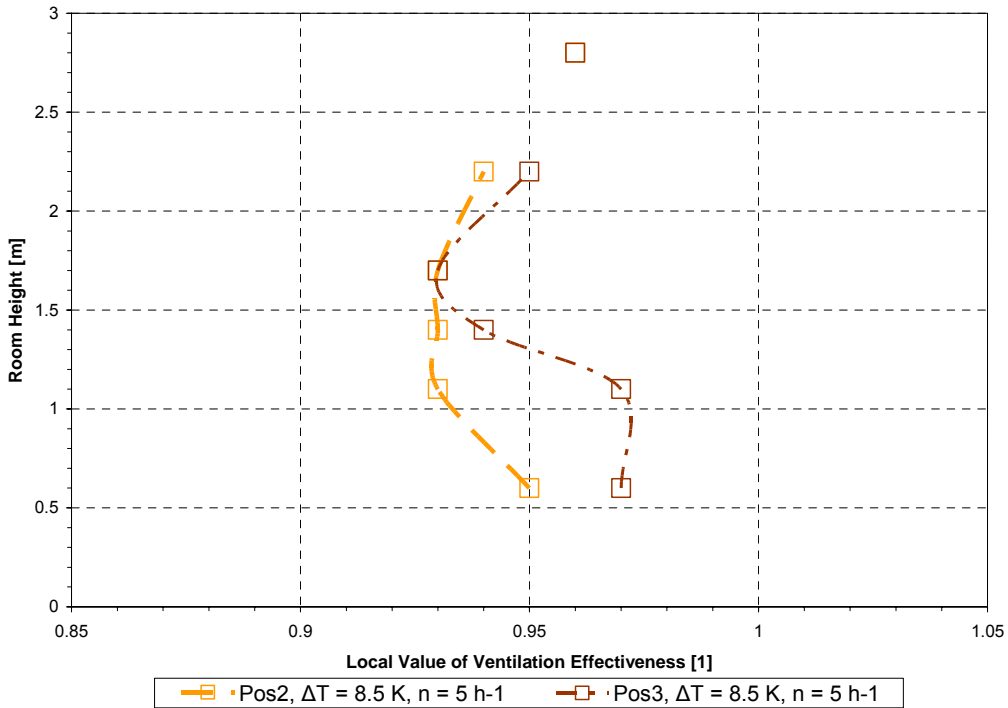


Figure 17: Ceiling Slots; Vertical Distribution of Local and Global Air Change Effectiveness on Position 2 and 3, IG=40 W/m²

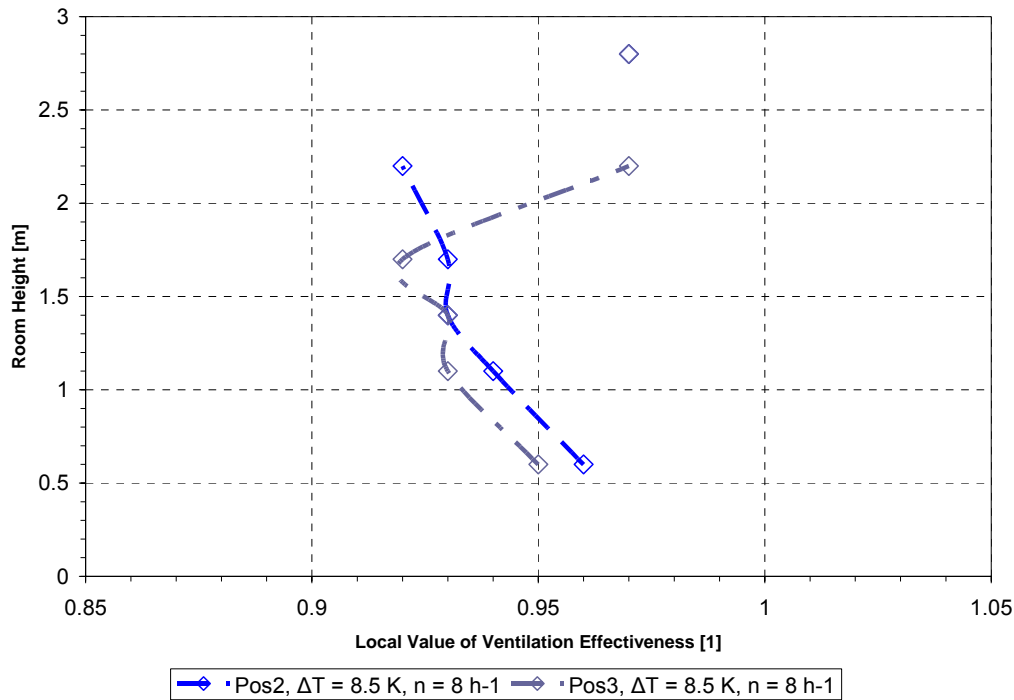


Figure 18: Ceiling Slots; Vertical Distribution of Local and Global Air Change Effectiveness on Position 2 and 3, IG=65 W/m²

Although the bandwidth of the results is small, it is also here possible to look into secondary flow patterns of the room by evaluating the local indices: Due to the arrangement of the slots, two circulation patterns going in the opposite direction can be found, which join each other again in the middle of the room. Near the ceiling and the floor, the air-exchange indices are slightly better than in the middle of the room. Furthermore, a suction effect could be found for internal gains of 20 and 40 W/m² due to the one-sided arrangement of the local heat sources in section 3 compared to the cooler air coming from section 1. This is reflected in the difference between the local indices of section 3 and section 1 ($\epsilon_{p\ 3-1} \approx 0.08$) and the temperature differences ($\Delta T_{3-1} \leq 0.5K$).

The design case ($n=8$ per hour with $\Delta T=8.5K$, Figure 19 and Figure 20) had an equal distribution of loads. The differences in temperature and local indices shown in the results are within the accuracy of the instrumentation. Comparing indices with temperatures just below the ceiling shows that the air-exchange is better in the cooler regions of section 1 and 3 than in the warmer part of the room, just below the air inlet section 2, where both circulations split up in the opposite directions.

Differences in indices and temperatures in the lighting fixtures are too low to judge for short-circuiting.

As already shown for ceiling twist diffusers, there is no difference between the air-exchange rate on the nose of the manikins or 0.3m in front of the manikin. Both

systems seem to destroy the boundary layer that is established through thermal buoyancy.

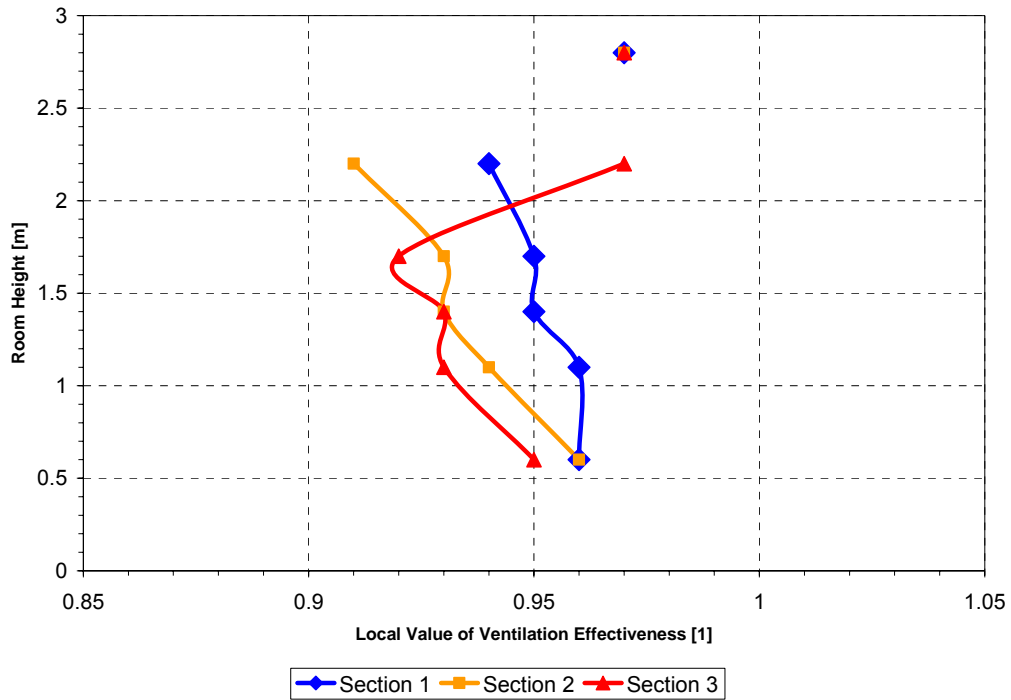


Figure 19: Ceiling Slots; Vertical Distribution of Local and Global Air Change Effectiveness at Sections 1, 2 and 3 for $n=8$ per hour and $\Delta T=8.5K$

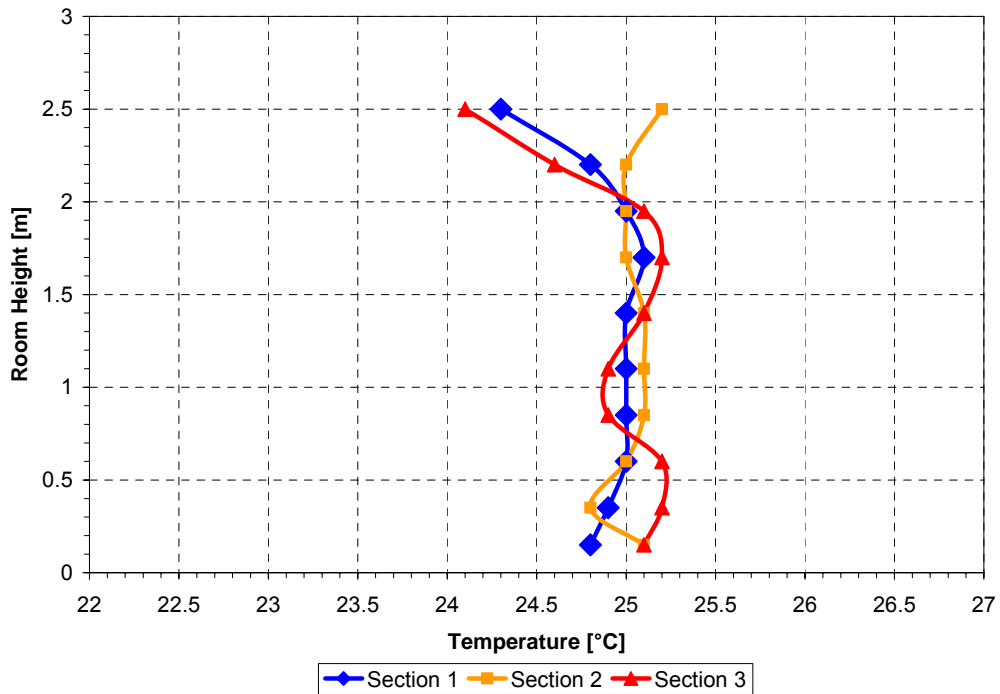


Figure 20: Ceiling Slots; Vertical Distribution of Room Air Temperature at Sections 1, 2 and 3 for $n=8$ per hour and $\Delta T=8.5K$

7.3 Floor Twist Diffusers

The amount and arrangement of the floor diffusers was changed during testing depending on the number of air changes per hour in order to achieve air flow rates per diffuser between 30 and $35\text{m}^3/\text{h}$ (18 to 21 cfm).

Tests without floor heating, i.e. total internal gains of 20 W/m^2 , resulted in air change values of about $\varepsilon_p=1.25$ to $\varepsilon_p=1.45$ up to the throw height of the diffuser, which was for all 3 air change rates about 1.1 m (see Figure 21). According to this, the temperature differences were small as well (from floor to 1.1m $\Delta T \leq 0.3K$).

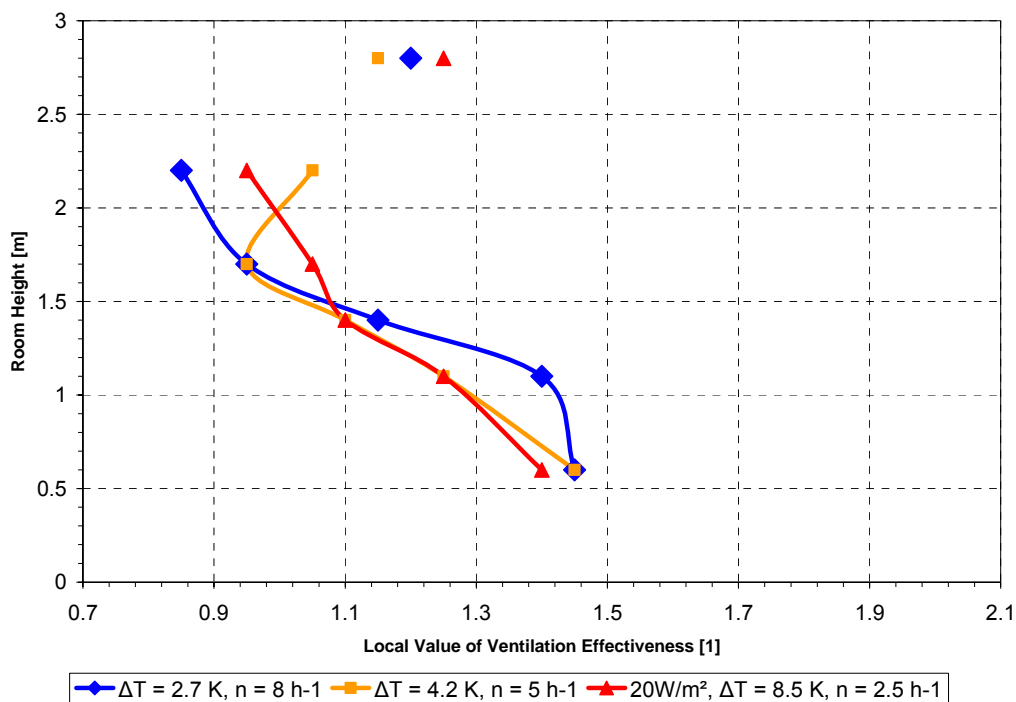


Figure 21: Floor Twist Diffusers, Vertical Distribution of Local and Global Air Change Effectiveness at Section 2 as shown in Figure 8 for 20 W/m^2 Internal Gain

For tests with internal gains of 40 and 65 W/m^2 , 50% of the total internal gain entered the room at floor height. Thus, an improvement in air-exchange was achieved within the occupied zone whereas the upper zone of the room resulted in similar air exchange rates. The global air-exchange indices turned out to be about 20% higher (see Figure 22).

For places that were outside the direct influence of local heat sources, therefore also influenced through thermal recirculation (sections 1 and 2), local indices <1 were partly found. However, this was in general only the case for places higher than 1.7m . Within

the occupied zone of the room, e.g. at section 3 and 0.3m in front of the nose of the manikins, respectively, the local air-exchange index was still 15% higher in the worst case for floor twist diffusers, than for the best case for entirely mixed systems (refer to Figure 23). When thermally driven buoyancy was increased (reflected in the temperature differences between return and supply air), the local air-exchange index at the nose of the manikins was considerably better than 0.3 m in front of the nose. This is because of the thermal boundary-layer that a person creates.

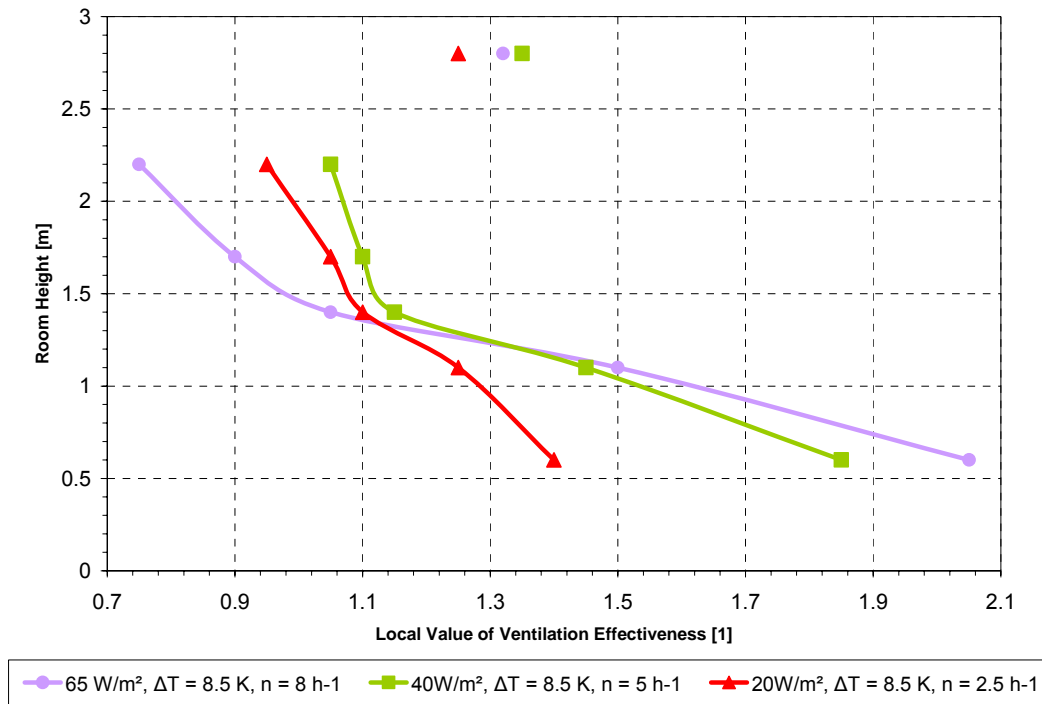


Figure 22: Floor Twist Diffusers, Vertical Distribution of Local and Global Air Change Effectiveness at Section 2 as shown in Figure 8 for 20, 40 and 65 W/m² Internal Gain

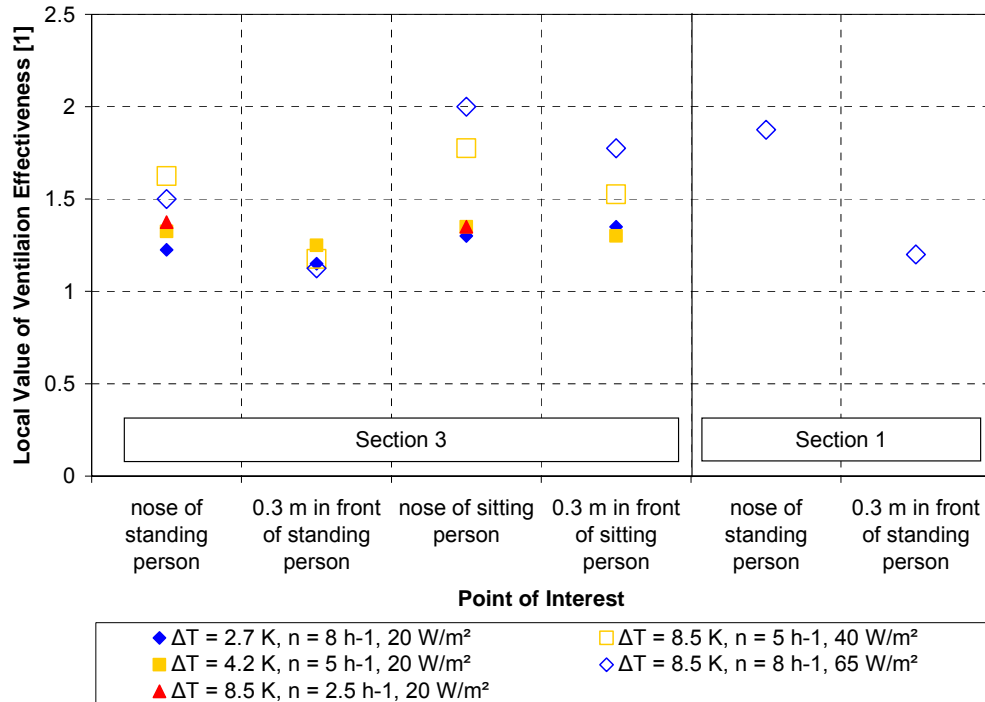


Figure 23: Floor Twist Diffusers, Vertical Distribution of Local and Global Air Change Effectiveness within the occupied zone of the room

This air distribution principle provides, compared to a displacement ventilation principle, in a positive sense, a distinctive demand-adapted behavior, which allows local heat sources and occupants, respectively, to be supplied with (cool) fresh air from the floor below. In addition, this is *independent* to the arrangement of heat sources and workstations within the room. However, it is advantageous to distribute the heat sources symmetrically in the room to achieve local air-exchange indices *throughout* the room. Walls have a significant impact: due to upward draft on the walls the air change is improved in this system. This was found for tests where the almost adiabatic walls had surface temperatures about 0.25K higher than the air temperature within the room. Downward draft would, however, decrease the air-exchange in the entire room.

In general, the already existing heat removal properties using [UFAD] could be verified and amended.

A comparison of the three vertical distributions of ϵ_p for the design case of $n=8$ per hour and $\Delta T=8.5K$ points out the displacement principle of this system (Figure 24 and Figure 25). The figures show that up to a height of 1.7m within sections with local heat loads the air change is better than outside these sections. Above 1.7m, the flow is characterized by thermal recirculation. The indices ϵ_p and the temperatures in the lighting fixtures show that recirculation is primarily in diagonal direction from room quadrant of light fixture B towards room quadrant of light fixture D: Air exhausted from light fixture B streamed in a displacing way through the occupied zone, due to the thermally driven buoyancy from the heat sources directly below the light fixture (light fixture B: ϵ_p is highest and shows highest temperature as well). On the other hand, the

exhaust air from light fixture D was cooled off due to mixing with air from the circulation path (light fixture D: ϵ_p is lowest and lowest temperature as well). Correspondingly, at section 3 the air exchange at 2.2m height is worse than in the other two sections 1 and 2. The other two light fixtures A and C show, in terms of air-exchange and air temperature, similar results as the general exhaust air properties.

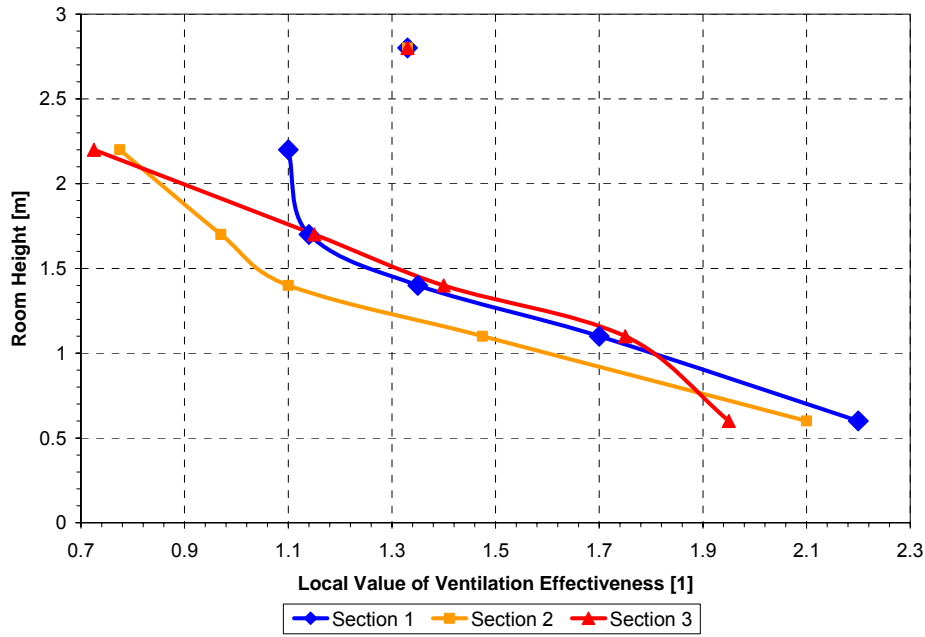


Figure 24: Floor Twist Diffusers; Vertical Distribution of Local and Global Air Change Effectiveness at Sections 1, 2 and 3 for $n=8$ per hour and $\Delta T=8.5K$

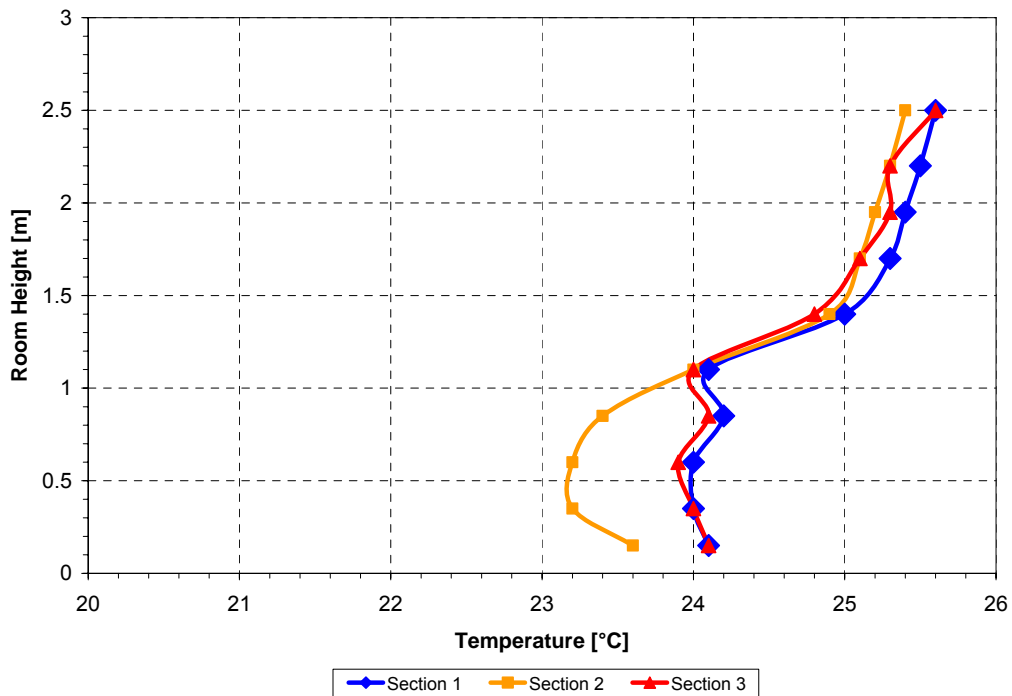


Figure 25: Floor Twist Diffusers; Vertical Distribution of Room Air Temperature at Sections 1, 2 and 3 for $n=8$ per hour and $\Delta T=8.5K$

7.4 Displacement Ventilation (DV)

The operation of a DV system is primarily governed by the thermal proportions within the room, i.e. the type and arrangement of heat sources and heat sinks and the resulting vertical temperature gradients.

The stratification height as typically found in DV systems was made visible with smoke tests and is very well identifiable through ε_p . Throughout the test series the stratification height was consistently between 1 – 1.4m. This small range can be explained as follows: The layer separating the upper and lower part of the room results from the balance between supplied airflow and the upward flows created from the heat sources. Small ΔT between return and supply air in relation to the internal gain would mean that the separation layer should be higher. At the same time, however, the resulting lower vertical temperature gradients also mean that airflow surrounding the heat sources increases by a multiple. Apparently, both effects compensate each other for typical room height in offices ($H < 3m$). A straight relation between the height of the stratification layer and the quality of air-exchange around the nose was not detectable, under the testing conditions applied, even for standing persons.

Furthermore, it is pointed out that only for a symmetric arrangement of heat sources *one* unique layer with a distinct height could be found. Testing conditions differing from symmetric heat source arrangement, especially the case with 20 W/m^2 internal gains, turned out to lead to lower separation layer heights outside the direct influence of heat sources.

Unlike floor twist diffusers, the local gradients of ε_p are much larger (Figure 26 and Figure 27). Firstly, this is due to the low-momentum introduction of supply air and secondly, because of the resulting low-turbulence upward flow created through the heat sources. Areas outside the direct influence of heat sources *and* above the stratification layer are therefore extremely influenced through thermal recirculation and result in $\varepsilon_p \leq 1$. In the occupied zone of people and heat sources, respectively, the air change was in general better compared to areas outside the direct influence of heat sources. For the surrounding air of the nose, the air-exchange indices turned out to even be much better (see Figure 28). Because heat fluxes created by people and office equipment as well as any other heat sources in the room (i.e. walls) are the only driver for displacement systems and cross-air-movements are very distinct due to the thermal layers in the room, local disturbances have a very strong impact on other parts in the room. This is not the case for turbulent air distribution systems which introduce supply air at higher momentums.

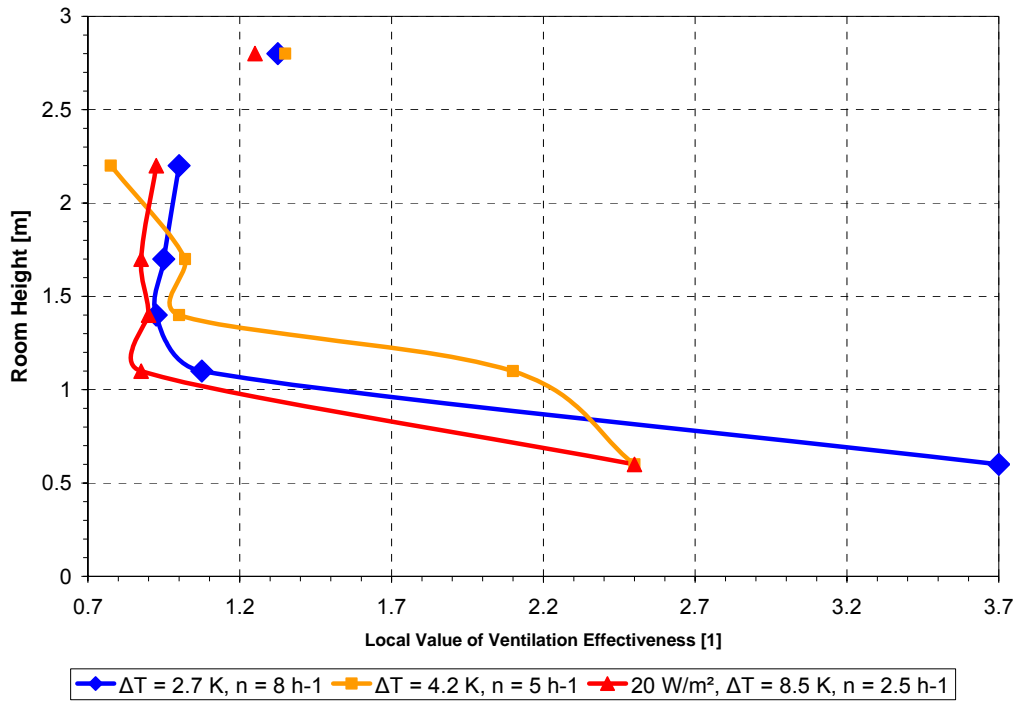


Figure 26: Displacement Ventilation, Vertical Distribution of Local and Global Air Change Effectiveness at Section 2 as shown in Figure 8 for 20 W/m² Internal Gain

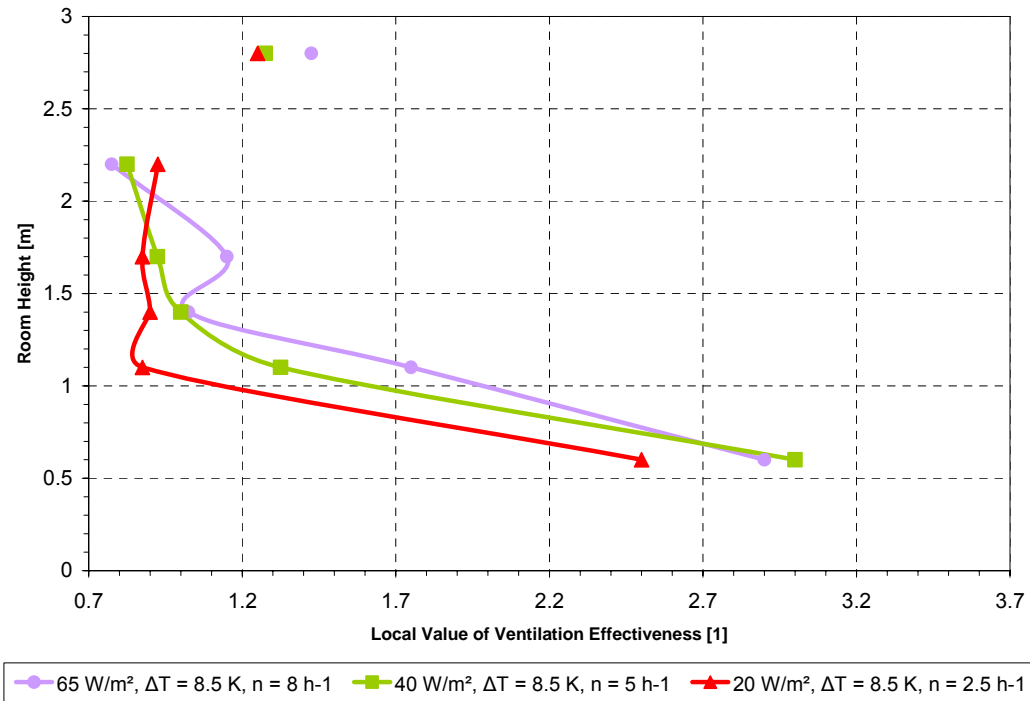


Figure 27: Displacement Ventilation, Vertical Distribution of Local and Global Air Change Effectiveness at Section 2 as shown in Figure 8 for 20, 40 and 65 W/m² Internal Gain

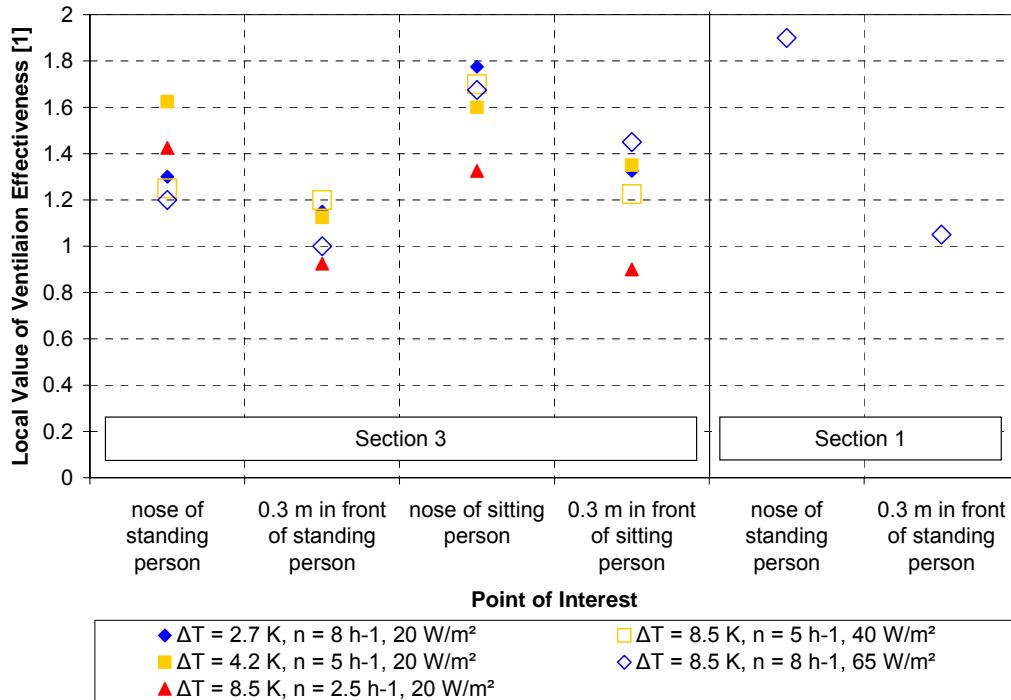


Figure 28: Displacement Ventilation, Vertical Distribution of Local and Global Air Change Effectiveness within the occupied zone of the room

In order to show how strongly DV systems rely on buoyancy driven flow, the impact of wall temperatures and local disturbances (e.g. computer fan) were studied for the case of $n=2.5$ per hour at 20 W/m^2 .

For the first test, the temperature of the environment of the test room was decreased so that the walls produced heat losses of about 25% of the total internal gain. Therefore the temperature difference between wall and room air was decreased from $+0.35\text{K}$ for adiabatic cases to $+0.1\text{K}$. By doing so, section 1 lost its influence on upward draft significantly (adiabatic environment resulted in $\epsilon_p=2.5$ to 4.0 across the entire room height right next to this wall). Thermal induced air change was now almost only driven by the one-sided arranged computers and manikins and decreased throughout the entire room above the stratification layer drastically. If the breathing zone of a person is above this layer, the air quality will primarily be determined by the interconnection of air from the thermal boundary layer and the re-circulating polluted upper zone air. In this case, the operation of a DV system strongly depends to which extent air and therefore pollutants from the upper zone enter the occupied zone of the room.

For this purpose, the effect of the computer fan was investigated in the second study. The fan produced an airflow of $50 \text{ m}^3/\text{h}$ (30 cfm) which significantly influenced the local air change around the manikins (total room airflow was $168\text{m}^3/\text{h}=99\text{cfm}$). Measurements next to the nose of the standing and sitting manikin in section 3 resulted in $\epsilon_p=3$ for computers where the fan was turned off. When the fan of the computer was turned on, the thermal boundary layer produced by the manikins was destroyed.

However, this only has a negative impact, if the local indices of the surrounding air are lower than $\epsilon_p < 1$. For the standing manikin there was no difference in decreased indices if the computer fan was blowing towards it or away from it, whereas for the sitting manikin only blowing towards it led to a decrease in air-exchange indices. This is due to the depth and stability of the boundary-layer *in front* of the nose of the seated manikin. Because of the upward airflow produced from the manikin's thigh, no difference in indices can be found up to a distance of 0.25m away from the manikin's nose. However, 0.15m left and right of the nose was already found to be outside the boundary layer.

Another source for disturbances which can influence the air quality within the thermal boundary-layer of the person is the act of breathing itself. The basic breathing volume of an adult without physical activities is about 0.5m³/h (0.3cfm) at a frequency of about 16 per minute. To investigate the impact of a person's breathing, one standing manikin was set up with two tubes simulating human breathing. The tubes drew off a *permanent* air flow of 1.5m³/h (0.9cfm). This value is equal to the amplitude of the inhaled air flow, if a time dependence of the form $\sin^2\omega t$ is considered (worst case). The air change effectiveness of the inhaled air dropped from 3.0 to 2.0 within the undisturbed boundary-layer. Therefore, breathing can be considered to have a marginal effect on the air quality. This was also found in recent research.

Comparison of the three vertical distributions of ϵ_p for testing conditions of $n=8$ per hour and $\Delta T=8.5K$ clarifies the effect of diminishing of loads of this system (Figure 29 and Figure 30). It further shows that above the stratification height only in areas with higher local loads the air-exchange indices are better than for ideally mixed systems.

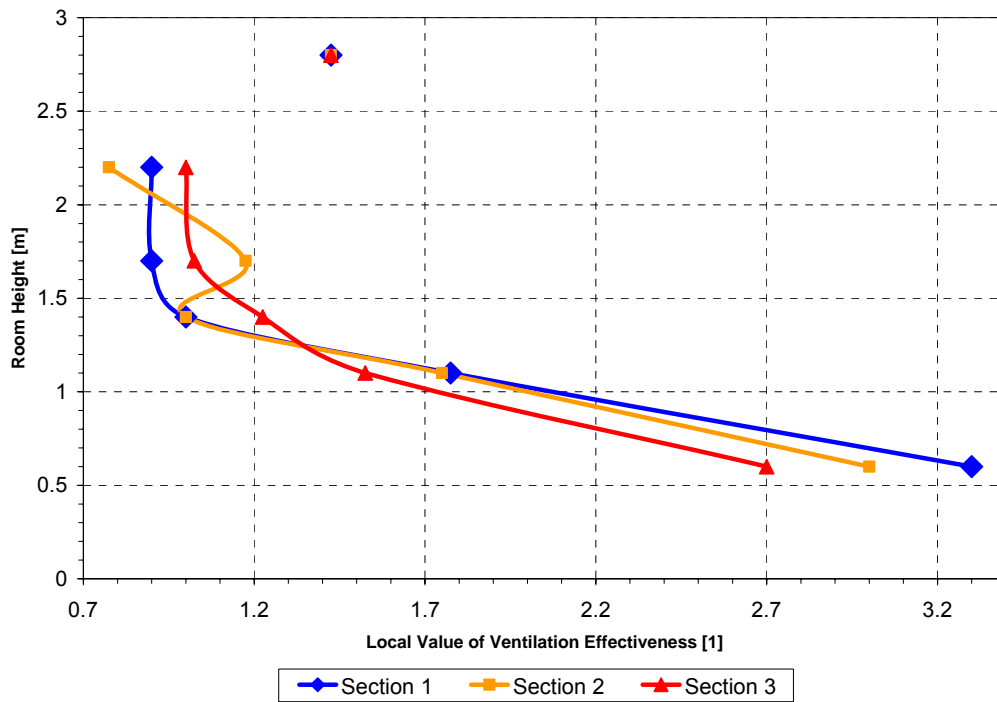


Figure 29: Displacement Ventilation; Vertical Distribution of Local and Global Air Change Effectiveness at Sections 1, 2 and 3 for $n=8$ per hour and $\Delta T=8.5K$

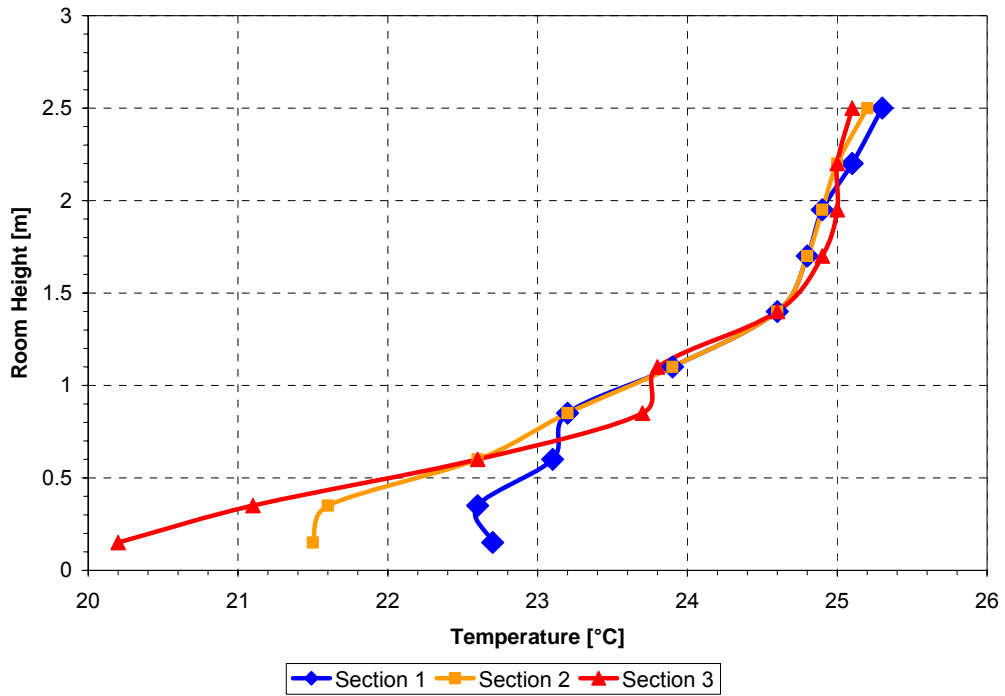


Figure 30: Displacement Ventilation; Vertical Distribution of Room Air Temperature at Sections 1, 2 and 3 for $n=8$ per hour and $\Delta T=8.5K$

In sections 1 and 2, the region above the stratification layer is characterized through recirculation. For all load cases tested, no specific flow pattern could be found, however.

The direction of how supply air is distributed within the occupied zone of the room can be identified very well by the local indices ϵ_p . In all load cases, the supply air spreads out over the entire floor towards the opposite wall and then reverses its direction towards the supply air inlets. This reverse-flow happened to occur on top of the flow towards the wall and established the separation layer to the area of recirculation. All points of measurements at 0.6m were within this layer. According to this direction of flow the values for ϵ_p decrease from section 1 to section 3.

Both standing manikins are surrounded with air of $\epsilon_p=1$, however, it seems that only for the manikin at section 3 the surrounding flow patterns are unfavorable. This leads to the point that more polluted air enters the separation layer and therefore decreases the air-exchange index in the breathing zone.

8 Conclusion

The developed tracer gas method for the 4 air distribution systems mentioned turned out to be a reliable and in practice usable process of evaluating the "age of air".

The measurement strategy consisted of cyclic sequence of step-up and step-down, in which the kind of tracer gas (SF₆ or N₂O) did not reveal any differences in results. For the evaluation of results, general applicable software was developed.

Using derived global and local air-exchange indices, which reflect the distribution of fresh air within the room, allows the quantification of, on the one hand, efficiency for air distribution systems and, on the other hand, the consequences of specific measures of air distribution techniques. The latter was demonstrated for ceiling twist diffusers and slots by two examples. Derived local indices give information about the entire room airflow pattern which was pointed out for all four air distribution principles by providing a detailed discussion of the local indices within each section. Such a detailed interpretation, however, demands the observation of flow patterns and measurements of air and wall temperatures.

Ceiling twist diffusers and slot diffusers create nearly mixed conditions. In both cases it is important to pay attention to the arrangement of air in- and outlets in order to prevent short-circuiting of the air. In practice, short-circuiting is associated with incomplete air-exchange. Both effects can be identified with the tracer gas method. However, separation of both is not possible.

Using floor twist diffusers and displacement systems significantly increases the supply of fresh air within the breathing zone of the occupants. Air-exchange indices are approximately 20 to 80% higher than for an ideally mixed system. The efficiency of a displacement system strongly depends on the arrangement of the heat sources within the room, the thermal proportion of the walls and the local flow characteristics around the occupants. Therefore, this system is much more sensitive to changes in any of the mentioned parameters in comparison to turbulent/mixing air distribution systems. In the case of proper arrangement and (adiabatic) operating mode, no significant differences in terms of local and global air change effectiveness could be found between displacement ventilation and UFAD systems.

Another important aspect is the proper removal of pollutants. This operation can not be evaluated by looking at air-exchange indices because the effectiveness of removal is not only depending on the room flow pattern but also on the type and arrangement of pollutant emitting sources. The relation between air-exchange and pollutant removal is part of continuing research.

9 Terminology

τ_p	age of air at point p
$\langle \tau \rangle$	average age of air of room
τ_e	age of air at exhaust
τ_n	nominal time constant
n	air exchange rate (air changes per hour)
ε_p	local air change effectiveness at point p
ε	global air change effectiveness
c_s	supply concentration
c_e	exhaust concentration
$c_{b,i}$	background concentration at point i
$\bar{c}_i(\infty)$	local end concentration at point i, maximum concentration
$\bar{c}_i(0)$	local start concentration at point i
$\bar{c}_i^*(t)$	measured concentration at point i at time t
$\lambda_i(t')$	degree of exponential decay at time t=t'
c_d	detection limit of gas analyzer
$\mu_i^{(m)}$	moments of time and dimensionless tracer gas concentration changes
$N_{s,max}$	maximum number of samples
N_{min}	minimum data density
Δt_{ana}	time of analysis
M_r	mass of air in the room
\dot{M}_s	mass flow rate of air in the supply duct
\dot{M}_e	mass flow rate of air in the exhaust duct

10 References

- [1] Sutcliff, H., "A Guide to Air Change Efficiency", Air Infiltration and Ventilation Centre AIVC, Technical Note 28, Coventry, Great Britain, 1990, Airbase #4000
- [2] Raatschen W., "Was ist Lüftungseffektivität?", Klima-Kälte-Heizung KI, Bd. 16 (1988), Nr. 5-8, Airbase #3094
- [3] Sandberg, M., "The Use of Moments for Assessing Air Quality in Ventilated Rooms", Building and Environment, Vol. 18 (1983), No. 4, pp 181-197, Airbase #1320
- [4] Esdorn, H., "Zur einheitlichen Darstellung von Lastgrößen für die Auslegung raumlufttechnischer Anlagen", Heizung Lüftung Haustechnik HLH, Bd. 30 (1979), Nr. 10, S. 385-387
- [5] Nordtest NT VVS 047, "Buildings-Ventilation Air: Mean Age of Air", Nordtest, Helsingfors, Finland, 1988, Airbase #2368
- [6] Presser, K.-H., Becker, R., "Mit Lachgas dem Luftstrom auf der Spur", Heizung Lüftung Haustechnik HLH, Bd. 39 (1998). Nr. 1, S. 7-14, Airbase #2883
- [7] Jung, A., Zeller, M., Raatschen, W., "An Improved Method to Determine the Age of Air from Tracer Gas Measurements", Proceedings of Roomvent '92, Pt. 3, pp. 231-244, Aalborg, Denmark, 1992, Airbase #6330
- [8] Axley, J., "Indoor Air Quality Modelling, Phase II Report, NBSIR 87-3661", US Department of Commerce, NBS, Githersburg, USA, 1987, Airbase #3418
- [9] Skaret, E., Mathisen, H. M., "Ventilation Efficiency – Part 2", SINTEF Report STF15, A84051, Trondheim, Norway, 1984, Airbase #2610
- [10] Grieves, P. W., "Measuring Ventilation Using Trace Gases", Brüel&Kjaer, Naerum, Denmar, 1989, Airbase #3884
- [11] Sinden, F., "Multi Chamber Theory of Air Infiltration", Building and Environment, Vol. 13 (1978), pp. 21-28, Airbase #5
- [12] Detzer, R. Jungbäck, E., "Bestimmung der Belastung des Aufenthaltsbereiches durch Wärme bei verschiedenen Luftführungen", Heizung Lüftung Haustechnik HLH, Bd 32 (1981), Nr. 7, S. 329-331

- [13] Dittes, W., Mangelsdorf, R., „Der Wärmetransport im Raum bei der Luftführung von unten nach oben“, Heizung Lüftung Haustechnik HLH, Bd. 32 (1981), Nr. 7, S. 265-271
- [14] Kofoed, P., „Thermal Plumes in Ventilated Rooms“, Ph. D. Thesis, Dept of Building Technology and Structural Engineering, Aalborg University, Aalborg, Denmark, 1991
- [15] Jung, A., „Messung der Lüftungseffektivität im Labormaßstab mit Spurengasen“, Heizung Lüftung Haustechnik HLH, Bd. 44 (1983), Nr. 7, S. 434-437, Airbase #6855
- [16] Recknagel, H., Sprenger, E., Taschenbuch für Heizung und Klimatechnik, R. Oldenbourg Verlag, München, 1981
- [17] Hyldgaard, C. E., „Humans as a Source of Heat and Air Pollution“, Proceedings of Roomvent '94, Pt. 1, pp. 413-433, Krakow, Poland, 1994